CRANFIELD UNIVERSITY

F MORTEL

CRANFIELD TEAM F1:

THE FRONT WING

SCHOOL OF ENGINEERING

CRANFIELD COLLEGE OF AERONAUTICS

MSc THESIS

CRANFIELD UNIVERSITY

SCHOOL OF ENGINEERING

CRANFIELD COLLEGE OF AERONAUTICS

MSc THESIS

Academic Year 2002-2003

F MORTEL

Cranfield Team F1: The front wing

Supervisor: P A RUBINI

September 2003

This thesis is submitted in partial fulfilment of the requirements
for the degree of Master of Science

ABSTRACT

Cranfield Formula 1 Team is a group design project composed of five students, each of them being responsible for the design of one part of the vehicle. The present thesis deals with the front wing design.

According to the time allowed to do the thesis and to learn the relevant software to use, three models were built: one is quite simple and is the basis of the two others. The aim was to design these three models using CAD (Catia V5, a product from Dassault Systems), to build their meshes using Gridgen (a product from Pointwise), to simulate the flow with Fluent 6.1 and finally to visualise it thanks to Fieldview 9.

The main aims of the different models are to deflect the flow from the wheels to reduce the drag created by the tyres and to create enough downforce taking care to match the FIA Formula 1 technical regulation. The design focuses on the endplates to fulfil these objectives.

Having done the CFD parts, the flow pattern was studied and the efficiencies of the different devices designed were assessed. It appears that the behaviour of the flow was greatly influenced by the front wheels (which were simulated with the front wing) as expected and therefore that the design has to take account of the environment of the front wing. The endplates demonstrate their utilities as deflectors that are able to suck the flow inboard the wheels. They also show that they can be additional downforce productive devices. The loads created there are not huge but are honest compared to the surface used and to the fact the design tested has been made without optimisation.

Finally, from the results of the simulation and the flow pattern obtained, many ideas come out to improve the efficiency of the front wing.

ACKNOWLEDGEMENTS

Dr Philip RUBINI
for his CFD advices

Jean-Marie "James" CAVET
for teaching me Gridgen

All my friends from Cranfield University for being who they are:
Audrey, Carine, Caro, Fabie (our fairy), Sophie, Véro,
Charlie, Florent (the tall but smaller one), James, Jérôme,
Markus, Nico, Pierre (for the breaks…), Robin, Seb and Steph.

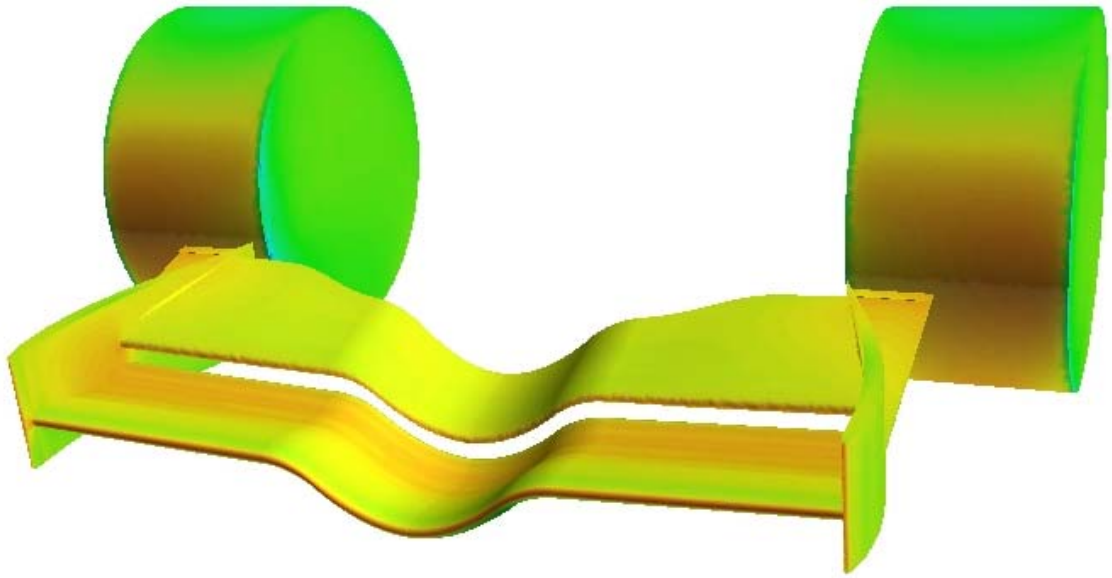

LIST OF CONTENTS

LIST OF FIGURES

INTRODUCTION

Cranfield Formula One Team is a group design project composed by five students: one from the Motorsport Msc, two from the Automotive one and two from the Aerospace Dynamics one.
The intention is for a common core of group and unique contribution from each team member. The members will have to work as a team as the design of some parts will influence the one from others. So, each design modification that may affect the design of an other part –it could be about the shape or about the aerodynamic parameters as parts of the vehicle would influence the devices downstream- should be discussed with the team-mates. This will be achieved by regular team meetings (every two weeks).

I chose to join this group because I have been fascinated by the Formula 1 aerodynamics field for a long time and by conception as I am keen on thinking about innovative devices.

My part of the work deals with the design of the front wing. From my aerodynamics background and from the previous front wings that make the Formula 1 cars go faster over the years, I set the design of different front wing geometries according to the 2003 FIA Formula One technical regulation and accomplished it using CAD (Catia V5, a product from Dassault Systems). Then, as the aim was to validate this design, it was decided to complete that step using CFD (Computational Fluid Dynamics) methods.

My principal objectives are:

- to match the FIA Formula One technical regulation.
- to study the endplates deeply, to use them as flow deflectors and as additional downforce productive devices.
- to create enough downforce.

I. LITERATURE REVIEW

This Literature review is based on the readings made during the thesis but most of the information provided comes from the readings I have made since 1991 as I have been passionate by Formula 1 since this time. In this way, some pieces of information are difficult to attribute or reference.

Some of the following front wing improvements quoted have been found too just by looking at the cars through the history in museums [1], books (as Ref.[2]) or magazines [3] and by seeing how they have evolved.

1. THE FRONT WING

The front wing is usually the first part designed by teams. Failing designing an efficient front wing may disrupt the whole aerodynamics of a Formula 1 car. Indeed the balance of the car is determined by the load on the front wing as the one on the rear wing is rarely modified on the track, the choice of the latter being determined by the track simulator before coming to the circuit. So the load on the front wing is required to be easily modified.

Nowadays the front wing is a two or three-element airfoil which is usually not anymore straight along its span. The main flap is usually a rectangular planform whereas the aft one could adopt a lot of different shape due to the flow constraints downstream. Then a Gurney flap may be fixed at the aft flap trailing-edge to gain some extra downforce. Finally, since the FIA Formula 1 technical regulation has constraint the teams to reduce the front track width of the cars, wing tips have become very complex due to the wheel-wing tip flow interaction.

2. AIMS AND OBJECTIVES

Formula One teams spent a lot of time and money designing the shape of their cars because of the importance of aerodynamics. Today the way to design a Formula One front wing is to try several features using CAD and CFD methods, to keep the ones that match the performance requirements for a specified track and then to evaluate the efficiency of the best ones in wind tunnels, the latter working 24 hours a day.

The front wing appeared in Formula One in 1968. It remains quite simple features with single rectangular airfoil with flat vertical endplates until 1990 when the front wing development started speeding up. This trend has become impressive since the middle of the nineties and especially since 1998 with the new generation of front wing tips.

The purpose of this thesis is to design the front wing of a Formula One car matching the 2003 FIA regulation.
A Formula One car can create downforce up to 1700 kg (2.8 times the mass of the car) on a low speed sinuous track like Monaco. The front wing contributes to generate 650kg on such a track at the highest speed the car can perform.
Then the aim of the front wing is to drive the air from its wing tips to the inside of the front wheels so that the perturbation caused by the latter may be reduced. This is done because the regulation allows building a front wing larger than the front track width minus the two tyres width.

The design has been done by thinking up to a design made from scratch and that may be innovative. This will be designed using CAD software. Then the model will be meshed and exported to CFD software that will calculate the flow characteristics around the front wing. Finally the results will be displayed using flow visualisation software.

So the aim of this thesis is to create a front wing:

- that may generate a load of around 600 kg at 330 km/h.
- that may be able to deflect as air as possible from the wing tip to the inside of the front wheels.
- to choose two suitable airfoil sections for the main wings.

3. OVERVIEW OF THE PAST FRONT WING DEVICES

Front wings appeared in Formula One on the Lotus 49B at the Monaco Grand prix on the 25th of May 1968.

However, the first inverted wing to be used to create downforce in motorsport was the one installed on the Chaparall 2E in 1966 [4].

Many Formula One constructors began to do the same thing and many wings flourished on the Formula 1 circus. The wings were fixed on the wheel hubs of the car to transfer the load directly to the wheels. This allows avoiding stiffening the springs of the suspension system that might create instability on undulating tracks. However the wings struts were not enough resistant and they sometimes broke.

Fig. 1: Lotus 49B (1968) [1]

The CSI (Comité Sportif International) was totally beyond the team's improvements. So it did not expect the emergence of the inverted wings. Moreover the teams went ahead by permitting the pilot to modify the incidence of the wings thanks to a pedal whether the car was in a corner or in a straight line.

But in 1969, the CSI modified the regulation:

- by prohibiting the mobile parts.

- by prohibiting the fixation of the wings struts on the suspension or wheels hubs.
- by limiting the wings width and the chassis height to one metre.

These decisions were taken for safety reasons as many wings struts failures occur as during the terrible 1969 spanish grand prix with the horrendous crash of the Lotus of Jochen Rindt and Graham Hill.

The teams then kept the same philosophy to design their front wing: a rectangular planform shape with endplates varying in shape and size as most of the aerodynamics improvements dealt with the underbody of the Formula One car.

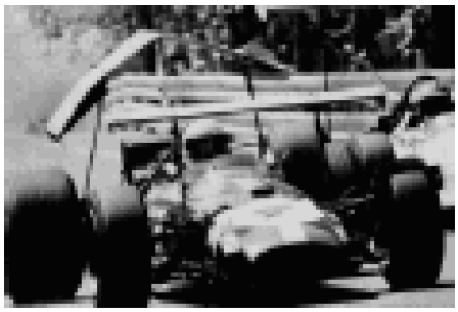

Fig. 2: Wing failure in 1969

In 1971, a new improvement appeared[5]. Bobby Unser was fed up with the Dan Gurney's car which was not quick enough. So he challenged Dan Gurney to come up with an improvement. The latter tried to fit a small spoiler at the trailing edge of the rear wing. In 45 minutes, the first Gurney flap was born and Bobby Unser tried it directly on the track. He was not faster but was surprised of the car was understeering. This was due to the new high-lift device: the Gurney flap.

Fig. 3: McLaren M23-5 (1974) [1]

This device is a flat trailing edge flap perpendicular to the chord and that is not longer that 5% of the chord (some new ones are not flat but are serrated). It

has been usually used at the front wing trailing edge to improve the load at the aft part of the second element (as if it is fixed at the first element, the flow would be disrupted and would not feed the second element's lower surface as well as it should).

A new way to wear the front wing was introduced by Ferrari with the 312 B3 in 1973: the front wing was worn quite far ahead from the body so that the wing-body interaction could be avoided but the ground clearance was quite high so that ground effect benefit was not achieved as well as it should.

Fig. 4: Ferrari 312 T2 (1975)

Innovations about the front wing were very limited during the end of the seventies as teams built wing-cars. Indeed the latter were so efficient that the front wing importance decreased.

McLaren MP4/1C (1983) **McLaren MP4/2 (1984)**

Fig. 5: Single element Vs multi-element airfoil[1]

New innovations were carried out when the two-element front wing was introduced in 1984. The angle of attack of the second element was allowed to be modified so that the load applied on the front wing could be changed as well as following the driver and engineer wishes. This second flap –whose chord was

not long at all in 1983 on the McLaren MP4/2- has then taken more and more importance as both its size and angle of attack were increased.

Fig. 6: Ferrari 640 (1989)

As the size of the second element has kept increasing, the shape of the latter changed by cutting it out near its root from 1989 on the Ferrari 640: the chord began to decrease from approximately the half span location to the nose. It permitted the second element to be set at a higher angle of attack without creating too much perturbation in the inside flow, without touching the nose that was still not raised in the late eighties and to keep the air to be diverted from the cooling inlets (for the engine).

Fig. 7: Tyrrell 019 (1990)

Then, in 1990 Tyrrell raised the nose of its 020 to increase the flow rate under the nose cone.

This lead to the Benetton B191 which wore a new high nose in 1991 that avoided any wing-body interference and allowed the front wing to be faced to the free stream all over the span. This permits to get a bigger surface to carry the load.

Fig. 8: Benetton B191 (1991)

In 1991 too, air deflectors were mounted behind the front wing tips to blow air behind the front wheels and so to reduce drag as wheels are the most important factors of drag on a Formula 1 car.

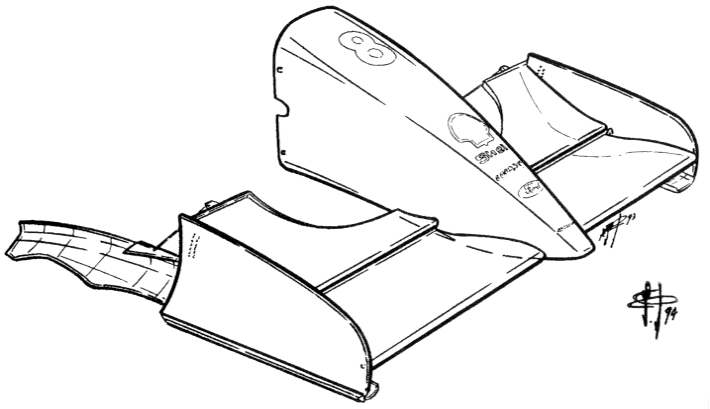

Fig. 9: McLaren MP4/8 (1993)[3]

Until 1994 and the Imola dramas which involved the death of Roland Ratzenberger and Ayrton Senna, the main factors that affect the front wing were the ground proximity and the presence of the front wheels.

After this event, the FIA Formula One regulation was modified and did not allow any chassis parts under a minimum ground height. This clearance was and is still different between the centre and the side of the car. Some of the ground effect was lost but more air flow can reach the cooling intakes. This allows the team to design multi-element front wing along the whole span without taking too much care to the air that will be provided to the side pods air intakes.
In 1995, to regain the lost ground effect, Minardi curved the front wing at the middle of the span of its M195 car as it was allowed by the regulation.

Fig. 10: Minardi M195 (1995)[3]

From 1998, the regulation decreased the front track width of Formula One car from 2 metres to 1.80 metre. However, the width limit of the front wing has remained equal to 1.40 metre. Thus, because of the tyres width, the front wing tips have been located in front of the tyres. To get the maximum load on the front of the car, teams have gone on keeping the front wing limit but had to design the front wing tips in a new way as the flow from the inverted wing interacts with the wheels. So two philosophies have been adopted: the first is to use the tip to drive the flow outward of the wheels and the second is to drive it inside of the wheels. The latter has become the majority trend as the inside of the tyres are closer than the outboard side.

4. DESCRIPTION OF THE FLOW AROUND THE FRONT WING

4.1 Flow over the wing span

The first element of the wing is a rectangular element. The flow around it is a classical flow around an inverted airfoil which benefits from ground effect. The latter is emphasized at the centre of the span as the regulations allow the team to build body device beneath 0.1 m above the reference plan (so between 0 and 0.1m) in an area that does not exceed 0.25 m from the centre line of the car (see Fig. 21). Indeed the flow may be curved inward at the location at which the airfoil is closer from the ground i.e. near the centre line (when it appears that the airfoil is curved downward there).

The first element incidence sometimes depends on the span location too: it is lower (quite null) near the tips so that the vortices that may be created there are lower. It is expected that the turbulence decreases behind the front wing.

Fig. 11: McLaren MP4/17 (2002) [3]

Then the first element provides air flow to the second element lower surface so that the latter's incidence may be increased at very high angle of attack (it can be more than 25 degrees).

The second element chord is usually reduced at the centre of the span to decrease the deflected flow downstream and to avoid interaction between the nose and the second element.

Finally a Gurney flap may be fixed to the aft flap trailing edge to increase the downforce in an easily and quick way. The Gurney flap causes a lower pressure area just behind itself which sucks the lower flow closer to the wing surface.

The Gurney causes some extra drag as well, but the wing can be run at a higher angle of attack and so can produce more downforce.

4.2 Flow at the tips

The tips' main aim is to deflect the flow from the front wheels (see for example the deflectors on the Ferrari F2002). The latter influence the air flow in a way that the air close to the tyre surfaces may be a reverse flow compared to the overall flow coming from upstream. There would be surface viscous effects too on the sides of the tyres but this may not be included in this study as this effects should influence the downstream flow rather that the front wing environment.

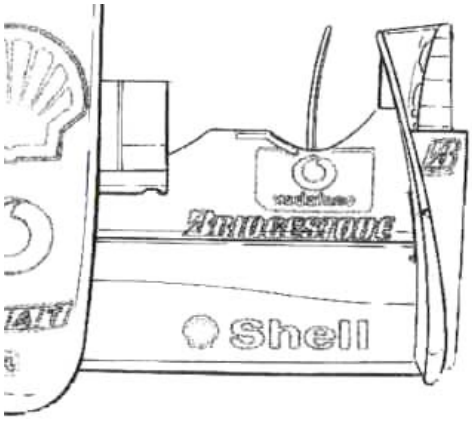

Fig. 12: Ferrari F2002 (2002) [3]

Fig. 13: Jaguar R3 (2002)[6]

Then, if the wing tip has an upper flat plate, a high pressure area can be created on it thanks to the viscous effect due to the rotating wheel if the horizontal surface carrying the load is sufficiently close to the tyre surface. Some horizontal surfaces may be designed as close as possible to the tyre surface (taking account of the fact the wheels have to rotate to permit the car turning) to create high pressure on their upper surface thanks to the rotating wheels.

Finally, in the last few years, as the regulation decreased the width track allowed, teams began to use the vortex lift (downforce in this case) on the front wing endplates.

5. MATCHING THE 2003 FIA FORMULA ONE TECHNICAL REGULATION

The design of today's Formula One car is constrained by the FIA 2003 technical regulation concerning the size of the body.

The design of the forward body is constrained by the articles 3.4, 3.6, 3.7 and 3.11 of the current technical regulation[7]:

Article	FIA Formula 1 Technical regulation
3.4	**Width ahead of the rear wheel centre line**
3.4.1	Bodywork width ahead of the rear wheel centre line must not exceed 1400mm.
3.4.2	In order to prevent tyre damage to other cars, the top and forward edges of the lateral extremities of any bodywork forward of the front wheels must be at least 10mm thick with a radius of at least 5mm.
3.6	**Overall height**
	No part of the bodywork may be more than 950mm above the reference plane.
3.7	**Front bodywork height**
	All bodywork situated forward of a point lying 330mm behind the front wheel centre line, and more than 250mm from the centre line of the car, must be no less than 100mm and no more than 300mm above the reference plane.
3.11	**Bodywork around the front wheels**
	With the exception of brake cooling ducts, in plan view, there must be no bodywork in the area formed by two longitudinal lines parallel to and 400mm and 900mm from the car centre line and two transversal lines, one 350mm forward of and one 800mm behind the front wheel centre line.
3.14	**Overhangs**
	No part of the car shall be more than 500mm behind the centre line of the rear wheels or more than 1200mm in front of the centre line of the front wheels. No part of the bodywork more than 200mm from the centre line of the car may be more than 900mm in front of the front wheel centre line.

The design of the forward part of the car is also influenced by the front wheels and the resulting flow around them.

The size of the wheels is constrained by the article 12.4 of the FIA technical regulation[7]:

Article	FIA Formula 1 Technical regulation
12.4	**Wheel dimensions**
12.4.1	Complete wheel width must lie between 305 and 355mm when fitted to the front of the car and between 365 and 380mm when fitted to the rear.
12.4.2	Complete wheel diameter must not exceed 660mm when fitted with dry-weather tyres or 670mm when fitted with wet-weather tyres.
12.4.3	Complete wheel width and diameter will be measured horizontally at axle height when fitted with new tyres inflated to 1.4 bar.
12.4.4	Wheel bead diameter must lie between 328 and 332mm.

As the regulation allows a short size self-starting capacity to the tyres manufacturers, the latter's data are necessary so that the design of the car could be completed. As a constraint, Michelin tyres for dry surfaces would be used. They are 350 mm wide and have an external diameter of 660 mm. They contain four longitudinal grooves of at least 2.5 mm imposed by the article 77 c of the sporting regulation[8]:

"c) Each front dry-weather tyre, when new, must incorporate 4 grooves which are :

- arranged symmetrically about the centre of the tyre tread ;

- at least 14mm wide at the contact surface and which taper uniformly to a minimum of 10mm

at the lower surface ;

- at least 2.5mm deep across the whole lower surface ;

- 50mm (+/- 1.0mm) between centres.

Furthermore, the tread width of the front tyres must not exceed 270mm."

All the size constraints from the FIA Formula One technical regulation are summarized on Fig. 21.

CONCLUSION

Considering the history of the front wing, all the devices that have already been tried and the environment of the front wing, a whole front wing including the tips will be designed according to the FIA Formula One Regulations.

The history shows us the way to follow as the past is the prologue to the future. So the designs implemented would be the results of the past front wings but have to try to bring innovative devices. It would then be assessed using CFD methods (mesh, flow parameters calculations, visualisation).

II. MODELS CREATION

The models were designed from scratch. This study focuses on the way to design the front wing and as the airfoils used for the horizontal multi-element wing are not current ones, the expected load on the front wing –around 2500N at 60 m/s- may not be reached even if the aim is to get as close to this amount as possible.

1. THE DESIGN

This part describes the different features contained by the different geometries built. The reason for designing the models in the way they are and the expected flow pattern around them are explained is the next section.

1.1 The basic Model

1.1.1 The multi-element airfoil

The basic element of a front wing is of course an airfoil. Nowadays, most of the teams use two-element airfoils even if some begin to use three-element airfoils for their front wing.

As I do not get any Formula One airfoil data, I used a GAW-1 airfoil for the first element as it has been used in the early nineties, the second being an airfoil section that have been used in an other motorsport area. The first element is set with an incidence of -1.5 degrees whereas the second one is set at 16 degrees.

The GAW-1 airfoil is designed as a rectangular wing of constant chord -the aspect ratio from the GAW-1 element being 5.4- whereas the second element chord is variable: it is shortened as the location is closed from the centre of the span. This is done to avoid any interaction with the nose witch dimensions are not already known.

Then, as the FIA Formula One technical regulation allows to decrease the ride height of any bodywork part at the centre of the span (until 25 cm from the centre line) to the reference plane, the decision of curving the wings at this location was taken to take advantage of the ground effect as much as possible. It should be noted that the ride height is not decreased along the whole length allowed by the regulation. This has been done to prevent a step in static

pressure at 25cm from the centre line and to permit the great depression at the centre of the wing to influence the pressure distribution along the whole span.

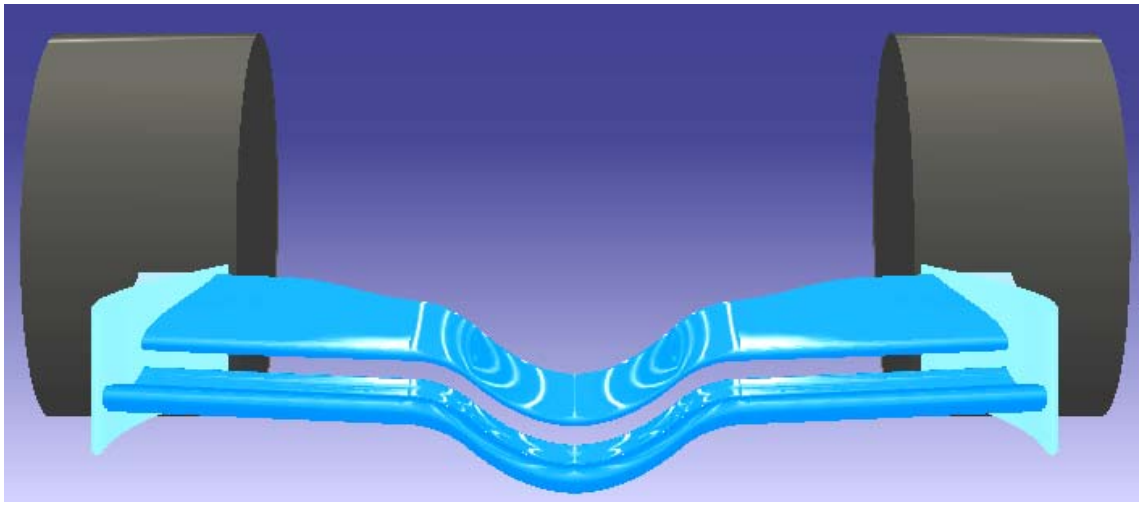

Fig. 14: The curved design at the centre of the span

At the tips, it was desired that the first element should be mounted higher to get a significant gap between its lower surface and the bottom of endplates. To fulfil this condition, the two elements are sloped along their span from the location at 25 cm from the centre line (at a height of 10 cm above the reference plane) to the endplates (at a height of 13.86 cm above the reference plane). This would prevent the air to round the tip as a great depression would suck the flow below the wing.

1.1.2 The endplates

The endplates have to be settled, according to the regulation, between 10 cm and 30 cm above the reference plane. This gap can be occupied by aerodynamics devices to deflect the flow inboard the wheels and to create additional downforce.

To deflect the flow, a thin vertical airfoil is introduced. It is referenced as NACA 68005 and is set with an incidence of 12 degrees.

It is a NACA 5-digit airfoil. The primary difference is the use of a different camber line. In a 5-digit airfoil, 1.5 times the first digit is the design lift coefficient in tenths, the second and third digits are one-half the distance from the leading edge to the location of maximum camber in percent of the chord, and the fourth and fifth digits are the thickness in percent of the chord.

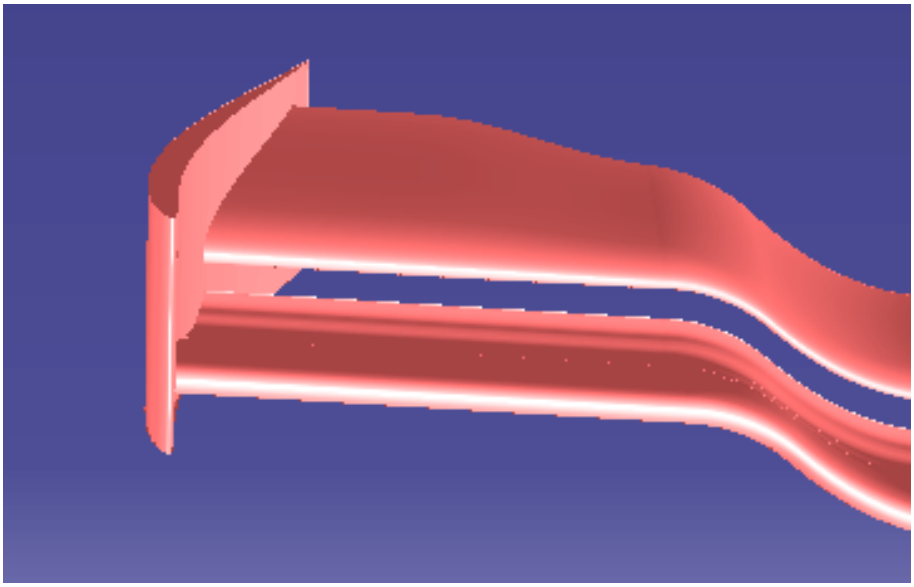

Fig. 15: The Basic Model

So here, the NACA 68005 has a design lift coefficient of 0.8, has the maximum camber at 0.4c and is 5% thick. Additionally, the first three digits indicate the mean line used. In this case, the mean line designation is 680.
The data of this section was created using the software "The NACA ordinate generation program V4.5-F" created by D.Lednincer and simplified by JC Etiemble.

This vertical airfoil is positioned so that the whole span allowed by the regulation is used and so that its trailing edge reaches the location at 55 cm from the centre line i.e. the inner face of the tyre. The flow inboard this vertical airfoil at its leading edge would of course be deflected inboard. Then, it is hoped that the flow should remain attached on the upper surface of the NACA 68005. It may be the case even if the stalling angle were reached as the air would have to round the wheel and so it would feed the upper surface (the outboard one) with enough air to prevent any separation.

This primary design sets a basic model of the front wing. Two models were born from the latter so that their efficiency might be compared. Building a basic geometry also permits to know the influence of the different part of the different front wings.

1.2 First Model

The first model philosophy is to deflect the flow inboard.

It contains:

-a vertical airfoil

-a second vertical airfoil

-an inclined flat plate

-an upper flat plate

The two vertical airfoils have been designed to deflect the flow inboard. The efficiency of the first big NACA 68005 is quite obvious (the same as the basic model one) but the one from the second small one has to be checked because of the wheel proximity. Indeed the wheel will make the air round itself quite efficiently. So the aim here is to deflect the flow before it reaches the tyre surface so that it would not create as superpressure as it would without this device. This would be hopefully done with an incidence of 20 degrees for the small NACA 68005 vertical airfoil. This may decrease the amount of drag generated by the wheels.

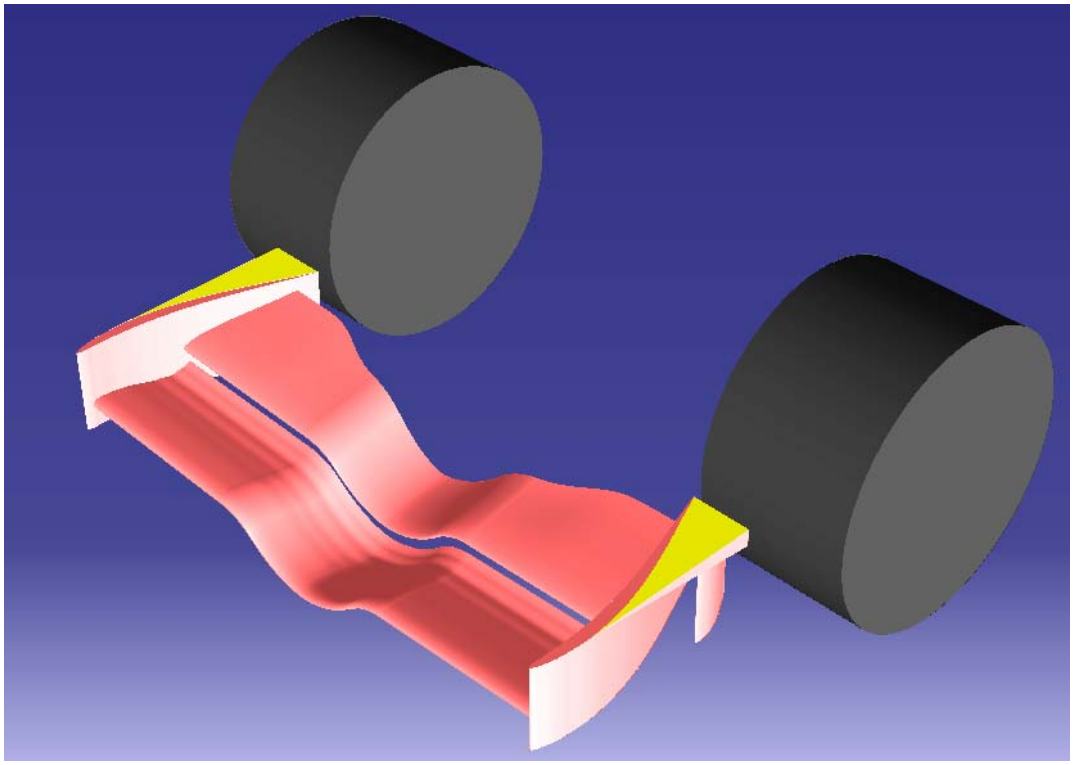

Fig. 16: The first Model

An upper flat plate has been added to take advantage of the induced flow from the rotating wheel.

Finally, an inclined flat plate has been designed to make the air go downward. Indeed it is easier to make air round the tyres close to the ground as the gap between the trailing edge of the big vertical airfoil and the tyre is higher at the lower side than at the upper side (as the tyres are round!). This would permit to deflect more air inboard the tyres, so to decrease the high pressure surfaces on the front side of the tyre and so to decrease the drag.

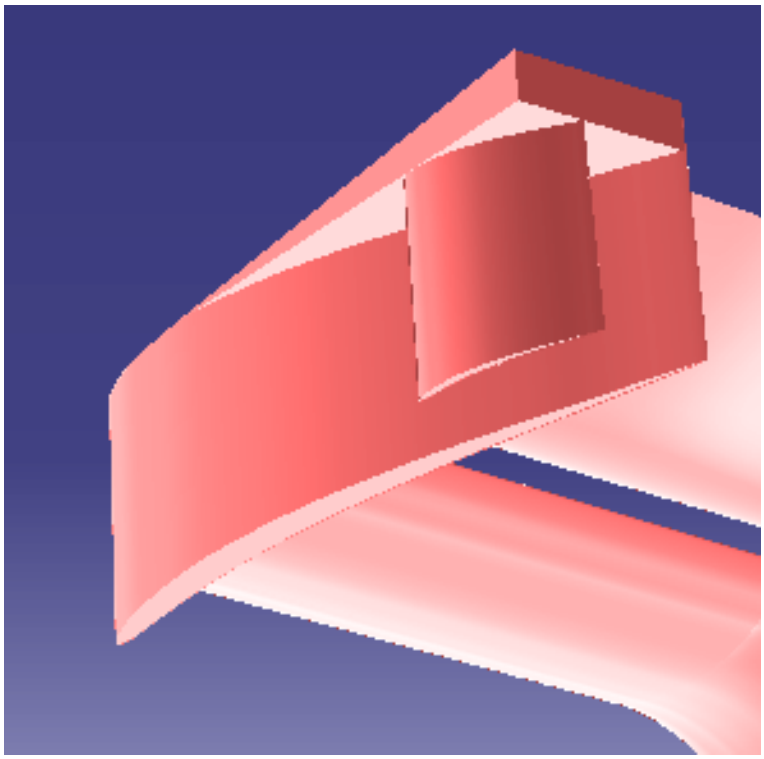

Fig. 17: The first Model endplate

1.3 Second Model

The second model has been designed to generate additional downforce (more than with the only flat plate from the first model) as well as deflecting the flow inboard.

It contains:

-a vertical airfoil as in the basic model

-a vertical airfoil which is smaller than the previous one

-a delta flat plate at 12° incidence
-an upper horizontal flat plate
-a lower horizontal flat plate

The two vertical airfoils have the same aim as the ones from the first model. The difference is that the small vertical airfoil is attached to a lower flat plate in the second model whereas it is linked to an upper one in the first case. Their size is different too: the first model's one extends along the whole height of the endplates whereas the second model's one has been cut off to avoid the destruction of the vortex under the flat delta plate. Their incidence is different: the big one is set to 12 degrees as for the basic and first model and the second one is set to 20 degrees as for the small NACA airfoil from the first model.

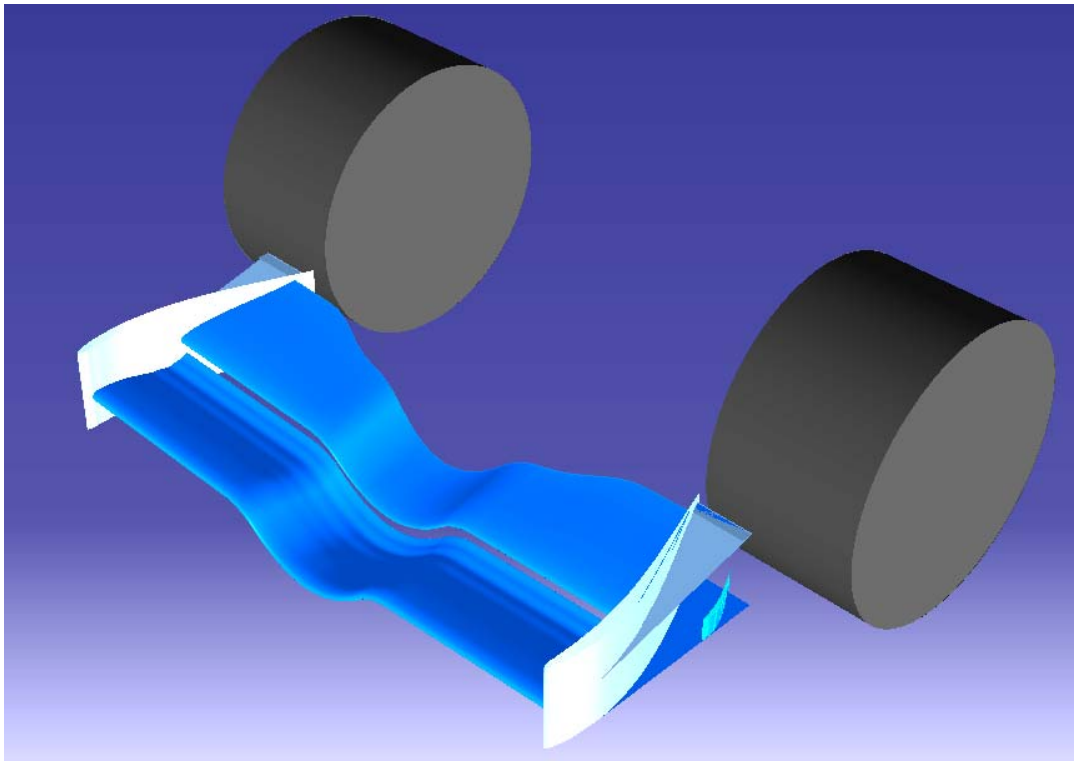

Fig. 18: The second Model

The delta flat plate has been added from the extreme allowed side of the endplate to the big NACA 68005. The aim here is to create a vortex underneath the plate so that the speed of the air increases inside them. The result would be a depression under the plate and so additional downforce. The incidence has been set to 12° thanks to results obtained during a wind tunnel session

attended with a student of the course (It should be noted that the delta wing used during these tests was not totally flat. So maybe this incidence should be refined).

Finally two flat plates have been added to take benefit of the resulted flow from the rotating wheel. The latter is due to the viscosity that makes the air close to the wheel go with it. So setting flat plates in front of the tyres allows catching the high pressure induced by this flow in order to create downforce. The additional downforce is not expected to be significant but it has to be checked as well as the interaction between the different aerodynamic devices and the flow rounding the tyres.

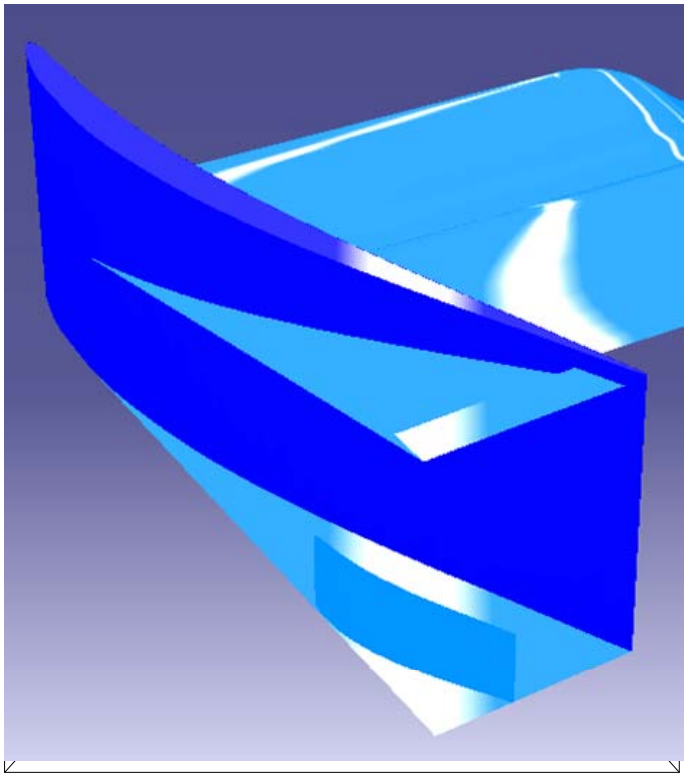

Fig. 19: The second Model endplate

This was the initial design, but as great difficulties occur during building the first grid, the lower flat plate and its small airfoil were removed for the following process. However, the effect from the small NACA 68005 would be highlighted by the simulation of the first model.

2. EXPECTED FLOW PATTERN

2.1 The multi-element airfoil

Because of the restrictions due to the FIA F1 technical regulation, the downforce needed has to be obtained with a limited surface. So, to get the right balance on the car, introducing a multi–element airfoil is required.

The first element sets a minimum amount of downforce and the second element is a movable part which angle of attack may be changed. In this way, teams are able to modify the balance of the car easily during testing sessions and grand prix.

The second element is used to being set at an angle of attack between 10 and 25 degrees. Separation does not occur as the first element feeds the lower surface of the second one with the air from its trailing edge.

No vortices are expected to be created with this two-element airfoil as it has not been set in the design aims of the whole car. Indeed, if a vortex is created there, it should be used downstream to create low pressure as the speed inside the core of the vortex would be higher. However, it seems that a flow that could be as clean as possible (without any vortex) should be expected. To avoid any vortex, the first element was designed as a rectangular planform and the modifications of the chord along the span were made smoothly for the second element. Indeed, if corners had occur along the span of the second element to decrease the chord, vortices would have been created.

2.2 Vertical airfoils

The aim is to get a thin and quite cambered airfoil which could be set at around 15 degrees without separation. The NACA 68005 is enough thin and is suitable to deflect the flow quite well without being too cumbersome (which is important because of the size restriction from the regulation).

2.3 Flow over wheels / Horizontal flat plates

The wheels are the devices that are responsible for the biggest production of drag: around half the drag of the car. Therefore the aim is to deflect the flow from the wheels so that the less air reaches the tyre surface.

Because of their shape and the fact that they are stuck to the ground, the wheels create lift[9]. Considering an infinite wide stationary cylinder, the flow pattern would be the following: the particles of air would be accelerated on the upper surface and would not be able to go through the lower one as the cylinder is assumed to be stuck to the ground. The flow would separate at around 160 degrees from the stagnation point. This means that the flow remains attached along a great distance and that the pressure coefficient becomes more negative on the upper surface because of the higher speed induced: in theory, the speed of air is doubled at 90 degrees from the stagnation point on the upper surface. This results in additional lift as it is the upper surface but it results too in additional drag as this negative pressure area is mostly located behind the middle of the wheel.
Then, as the wheel rotates, the separation point goes forward. This destroys the original lift generated by the wheel and the drag generated by low pressure surface too. However drag is very high because of the separated flow behind the wheel.

About the flow pattern, the wheels modify the flow due to their rotation. In front of them, the flow tends to go down and the stagnation point gets closer to the ground as the rotation speed increases. So the flow separates in two sub flows at the stagnation point. The lower one is confronted to the wheel in front of it and to the ground below it. A recirculation area forms and the flow escapes on the sides.

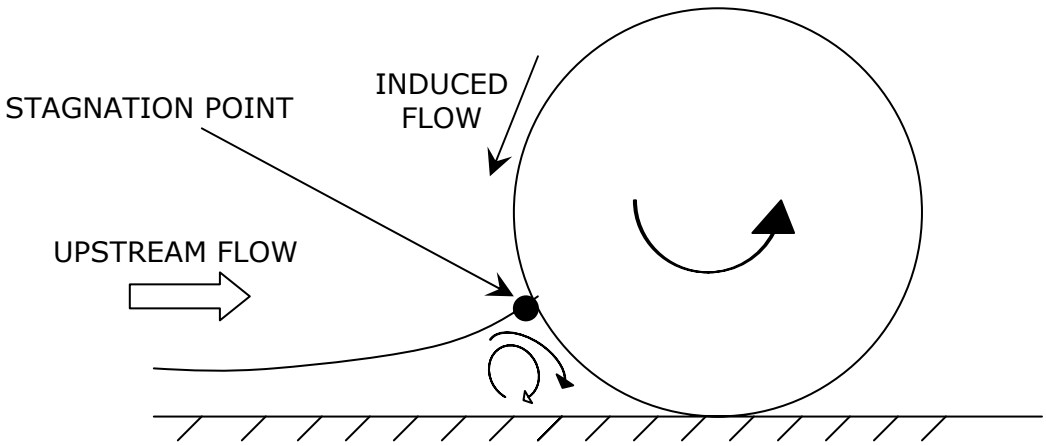

The aim is to take benefit of this induced flow by adding horizontal flat plates. The more they are located close to the ground and the wheel, the more additional downforce generated by the high pressure in this region. Downforce is there created by the fact the plates in this region would be hit by the air coming from the top and so, high pressure area would be created on their upper side.

2.4 Inclined flat plates

Whereas airfoils aim is to maintain the flow attached to generate downforce, the latter can be produced by making the flow separate. This is done by using flat plates utilising the vortex lift.

The flow is expected to separate at the leading edge (or apex in our case) which has to be very sharp. This phenomenon occurs at very high angles of attack as the flow would remain attached if the plate is not enough sloped.

In our case, the plate is a delta-shaped wing with an external boundary parallel to the main flow direction (view from the top) and with the internal edge stuck to the main vertical airfoil surface. Of course, this plate has a negative angle of attack to create a vortex under the plate.

In our case, the flow would separate along the edge of the plate and develops on the lower surface. The layers of air would mix and form a free shear layer that rolls down in a concentrated spiral vortex. Its thickness increases with the distance to the apex.

This strong vortex induces high speed and low pressure upon the vortex core. So the low pressure area is located under the flat plate and so downforce is created. On a traverse section, the pressure reaches a minimum value at the axis location of the primary vortex. Indeed, the primary vortex born from the separation of the boundary layer at the side edge of the plate can induce a secondary vortex.

Such a vortex (the primary one) can burst if the angle of attack is too high and the burst point moves upstream by increasing it.

However the flat plate used on the second model of the front wing would be short enough to prevent vortex bursting. But the vortex will certainly be disrupted by the flow induced by the rotating wheel or by the superpressure in front of the tyre.

The drag penalty of this kind of device is significant and is higher than the one from an airfoil but it is not really important here as the vortex goes downstream in the direction of the tyre and may be destroyed by the latter. Anyway, the drag penalty from this device can not increase the drag significantly as the tyre already fulfils this "mission". So the location of this sloped flat plate is particularly adapted.

III. SIMULATION

1. Modelling

1.1 Models

The models have been done with Dassault Systems Catia Version 5. A basic model with the two-element airfoil and the vertical airfoil as an endplate was first tested as the geometries from the other designs were more complicated.
Then the first and the second model were designed. However, the second model was truncated as the edges provided by Catia were not suitable for Gridgen. This problem highlights the huge importance of designing the model for the grid generation software, so by cleaning the geometry as much as possible. In this case, the geometry was cleaned but it was not enough. So as the time allowed did not permit to spend more time on the Dassault Systems software, the small NACA 68005 and the bottom flat plate were removed. This is not that important as the efficiency of this kind of small airfoil is included in the first model.
Half of every model was done for each simulation and they were then duplicated by symmetry for the flow visualisation.

1.2 Wheel

Real alloy was not designed as it would have been too time consuming because of its design, the additional mesh refinement it would have required and so the increased time of simulation.
So for each model, the wheel was designed as a 330 mm diameter and 350 mm large wheel. These dimensions match the regulation and are the same as the ones picked by Michelin this year[10].
The wheel was slightly buried of 5 mm to simulate the tyre deflection and give a consequent contact patch between the tyre and the track. Then this permits meshing easily as the edges would have been too sharp otherwise. However, a way to improve the model might have been to replace this sharp corner (between the tyre tread and the ground) by a fillet.
Finally, the wheel was set without any camber.

2. Grid Generation

The grids were done using Gridgen[11]. The first one for each model was done without boundary layers as the aim was to carry out an inviscid simulation before a viscous one.

2.1 The boundary layer

2.1.1 The Y+ parameter

At the wall in a turbulent boundary layer the no-slip condition requires that the speed is equal to zero at the wall. As the Formula One car average speed is around 55-60 $m.s^{-1}$ (around 200 km/h), the Reynolds number dealing with the front wing are from 10^6 to $3x10^6$ (depending on the device picked on the front wing). So the flow would definitely be a turbulent one at the front wing surfaces.

To investigate the wall region, a characteristic non-dimensional distance from the wall is introduced. It is called the wall unit (y^+) and is defined by:

$$y^+ = y.\rho.U_\tau / \mu$$

with:

ρ= volumic mass of the air (=1.225 $kg.m^{-3}$)

μ= dynamic viscosity (=$1.8x10^{-2}$)

$U_\tau = (\tau_w/\rho)^{0.5}$ which is the friction velocity

The boundary layer may be divided in three parts:

- a laminar sub-layer with $y^+<5$
- the blending region with $5<y^+<30$
- the log-law region with $30<y^+<1000$

the first two ones being named "viscous sub-layer" too.

In the laminar sub-layer, the turbulent shear stress is negligible. The shear stress is essentially but not totally laminar and velocity gradient is determined by viscosity. In the blending region, viscous and turbulent stresses have similar magnitude.

And in the log-law region, the flow is still dominated by wall but viscous effects are now negligible.

2.1.2 The viscous model mesh requirements

The Spalart-Allmaras model is a low Reynolds number model. It is designed to be used with grids that resolve the viscous region. The turbulent viscosity is attenuated in the viscous sub-layer thanks to functions built in the Fluent code. So to use the Spalart-Allmaras model efficiently, the wall treatment should be enhanced obtaining a y^+ value close to 1 although y^+ values up to 4-5 are acceptable.
However a coarser mesh should be run properly with the Spalart-Allmaras model thanks to the log-law which is valid for y^+ values between 30 and 60.

2.2 Building the grid

Even if building boundary layers with Gridgen is quite simple, doing this on every surface was quite impossible as the boundary layer's blocks were interacting the one with the others. It was so decided to build a boundary layer just on the two-element airfoil and on the front side of the wheel as it should be interesting to see the induced flow from the rotating wheel. However, the resulted grid contains some (at least one!) negative volume. It is certainly due to a volume built with cells with bad aspect ratio but even if the aspect ratio range of the grid was largely decreased, the negative volume has never been found.

To prevent the model from including negative volume(s), the decision was taken to build a quite coarse grid and then to refine it using the adaptation tools from Fluent.

So for all the models, after a first k-ε solution, it was determined that y^+ values of the cells on the wall boundary were too large and y^+ adaptation was used to refine them.
So to get a suitable mesh for the viscous flow calculation, it was decided to adapt the grid from the inviscid and k-ε viscous solver simulation thanks to the ability of Fluent to incorporate solution-adaptive refinement of unstructured mesh. By using solution-adaptive refinement, cells can be added where it is needed in the mesh, thus enabling the features of the flow field to be better resolved. This permits too to use the computer resources more efficiently. Here is the enormous advantage of creating an unstructured mesh: it appeared that

building a coarse mesh with Gridgen and then refining it with Fluent was the best method to get a better accuracy where it is needed.
The procedure is the following:

- First, a coarse grid was generated with Gridgen.
- Then it was exported to Fluent.
- A new simulation –which used the k-ε viscous solver- was directly run or was started using the converged solution from the inviscid one when needed.
- Then, when it converged, as the k-ε solver interpolates the boundary layer, the grid was refined using the y^+ adaptation method from Fluent.
- Finally the calculation went on using the Spalart-Allmaras viscous solver which is more suitable for airfoil simulation (or first with the k-ε solver).

Badly, even if the height of the cells along the wall boundary has been reduced during the refinement process, the refinement provided by the y^+ adaptation from Fluent did not allow to get an expected value of $y^+<5$ for the whole models, or at least for the different front wings because of the restriction of memory set by the software and by the computer.
For example, an original grid contained around 330000 cells. After a first refinement, around 200000 cells were added. Although it decreased the y+ values, the latter were still too huge compared to the expected mesh. So a second refinement was tried but Fluent crashed because of lack of memory available. This experiment was done at least ones for the three front wings without any success. Finally, it was decided to keep the coarse grid (with one adaptation) to get at least a suitable comparison between the different models.
These (one for each model) coarse grids are in fact 500000 to 750000 cells original grids that are refined once using the adaptation process from Fluent. These ones make the grids reach around 1200000 cells. Fig. 22 and Fig. 23 show the density of cells on the front wing surface and on the plane at 0.4 m from the leading edge.

So the meshes used can not be properly done to get the best results with the Spalart-Allmaras viscous model. The k-ε solver would also be used to compare the different viscous models.

3. CFD simulation

The CFD simulations were carried out with Fluent 6.1[12]. The latter is a solver of the Navier-Stokes equations.

2.1 The solver

The first simulations were done using a segregated solver and were inviscid flow calculations.

2.1.1 Viscous solver

However, the aim was to carry out viscous simulation to get evidence of the strong impact of both a moving ground and a rotating wheel.

The Spalart-Allmaras viscous solver seemed to be the most suitable solver for this kind of study. However this viscous solver did not converge for all the models. So the decision was taken to run the several models first with the inviscid or k-ε (with standard wall functions and then -sometimes- with the enhanced one) solver and when it has converged, to switch to the Spalart-Allmaras one. This was not a real problem as it matches the grid generation and adaptation refinement strategy. Many attempts were done with k-ε (both standard and enhanced wall functions, the enhanced one with the pressure gradients option), k-ω (SST with the transitional flow option) and Spalart-Allmaras.

The basic model and the second one converged easily with the k-ε viscous model but did not with the Spalart-Almaras one. Weirdly, it was the reverse situation for the first model.

2.2.2 Calculation solver

All the calculations were done using a first order SIMPLE model. No attempt were done with any second order solver as the simulation with the first order one were already too time consuming because of the size of the mesh used.

2.2 The boundary conditions

Nowadays the average speed of Formula One car over a lap can be from 150 km/h to 240km/h. In this way, a speed of 60 m/s (216km/h) has been set for the study.

The boundary conditions have been set as follow:

-the inlet of the domain:

The flow upstream of the front wing is not disrupted by the other devices of the car even if the flow may be disrupted if the car follows another one.

So the inlet was set as "*velocity inlet*" with an intensity and length scale turbulence type:

-the airspeed at the entrance is equal to 60 m/s.

-the turbulence intensity is set to 3% which is a standard value recommended (to get suitable results for the wheel (see the Analysis part), other turbulence intensity (down to 0.1%) coefficients were tried but the results did not change as expected).

-the length scale is set to 0.3 m which is the average length of the chord of the two airfoils from the two-element wing.

-the front wing:

Set as a "*wall*", of course…

-the ground:

set as a moving "*wall*". Its speed is equal to the air velocity inlet one: 60 m/s.

-the wheel:

set a moving "*wall*". The wheel was built as a cylinder and rotates around its axis at 181.82 rad/s so that it is equal to a speed of 60 m/s on the track.

-the outlet of the domain:

set as "*outflow*".

-the sides of the domain:

set as "*symmetry*". It is obvious for the side that deals with the centre of the car as the latter was split into two sections. For the other ones, the fact they are far enough from the front wing and because of the "symmetry" boundary characteristics –that are that the velocity vectors are parallel to the flow- permits to set them as "symmetry" boundaries.

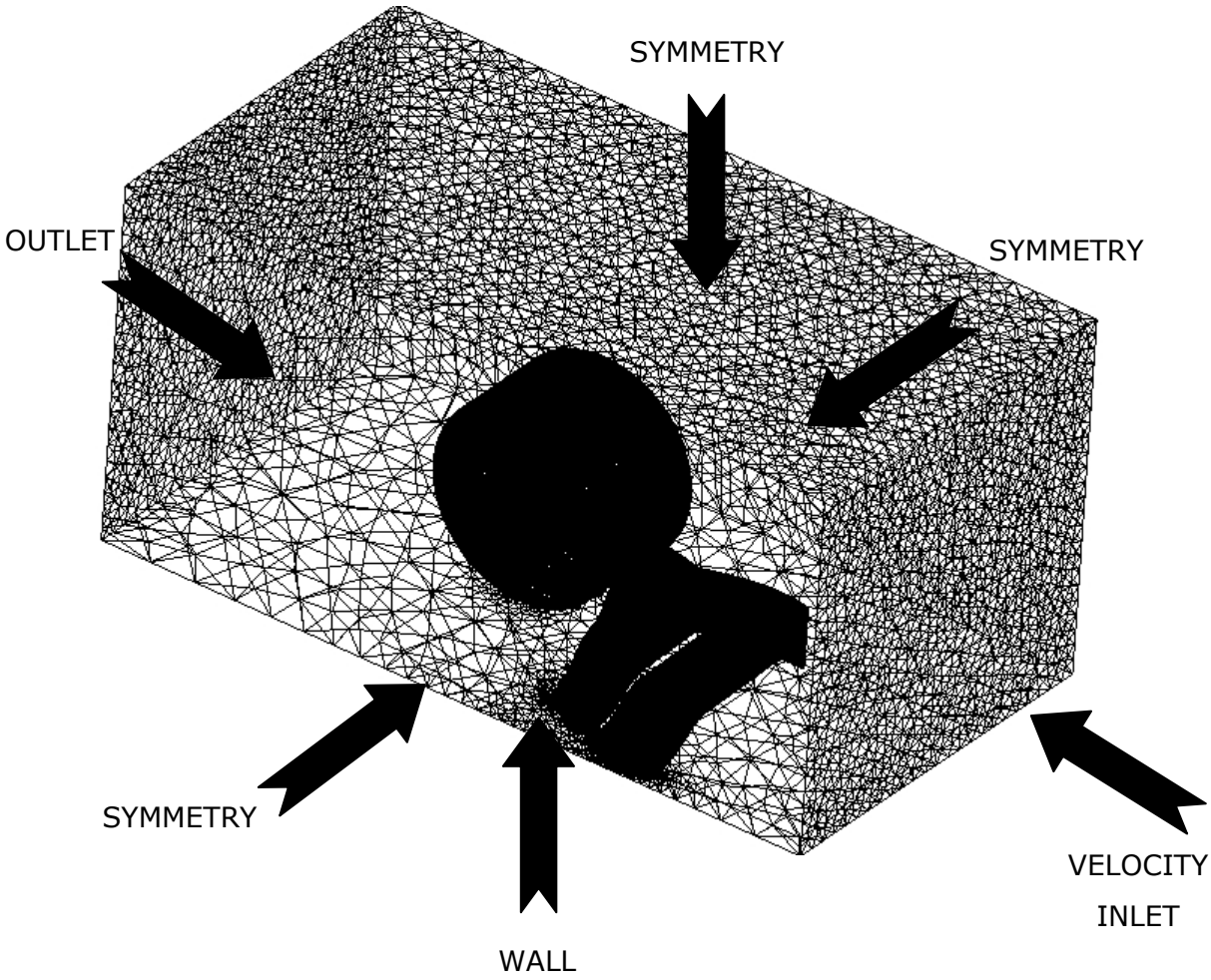

And of course, the front wing and the wheel are set as WALLS.

IV. ANALYSIS

The analysis is based on the flow visualisation provided by Fieldview 8.2 and 9 with the results from Fluent 6.1.
Thanks to Fluent, the C_L and C_D values were calculated too but they are not the primary concern of this study whose aim is to get more information about the flow around the endplates of a Formula One front wing.

1. FRONT WING PERFORMANCE

The reference surface that have been used to get the C_L, C_D and forces values are the following:

Model	For the Lift		For the Drag	
	Front wing	Front wing and wheel	Front wing	Front wing and wheel
Basic	0.331 m^2	0.561 m^2	0.095 m^2	0.325 m^2
No.1	0.354 m^2	0.584 m^2		
No.2				

These reference surfaces are the ones that have been estimated from the Dassault Systems Catia V5 software.

At 60 m/s, the results obtained are the following:

Model	Viscous solver	Lift		Drag	
		C_L	Force (N)	C_D	Force (N)
Basic	Inviscid	-1.40	-2056	0.55	228
	k-ε	-1.29	-1882	0.64	268
	Spalart-Allmaras	-1.26	-1836	0.57	238
No.1	Spalart-Allmaras	-1.20	-1872	0.66	278
No.2	Inviscid	-1.34	-2100	0.56	236
	k-ε	-1.23	-1920	0.66	276

The results obtained are below the expected ones that were at around 2500 N for the downforce. However it could be sufficient regarding the fact that the airfoil sections used for the multi-element wing –that is responsible for most of

the downforce created on the front wing- are not current Formula 1 airfoils sections but are some that were mounted on the early nineties Formula 1 cars.
Looking at the results, it can be stated that there is quite no difference between the different results. However, the most efficient in term of downforce is the Model 2 that provides around 40N more than the basic model according to the CFD calculation (the contribution of the additional device, the inclined flat plate, is easier to attribute when the second model is compared to the basic one). This difference is due to the inclined flat plate that provides the vortex lift.
Then in term of drag, the difference is insignificant as there is less than 10N between these two models.

Here are the calculations including the rotating wheel:

Model	**Viscous solver**	**Lift**		**Drag**	
		C_L	**Force (N)**	**C_D**	**Force (N)**
Wing*	Spalart-Allmaras	-0.11	-280	1.31	1794
	k-ε	-0.13	-308	1.36	1886
Basic	Inviscid	-0.28	-682	1.32	1898
	k-ε	-0.26	-634	1.37	1964
No.1	Spalart-Allmaras	-0.26	-676	1.30	1860
No.2	Inviscid	-0.29	-736	1.32	1898
	k-ε	-0.28	-720	1.32	1904

* "Wing" is the two element wing without endplate.

The results concerning both the front wing and the wheels are very interesting as they highlight the benefit from how the downstream flow comes from the endplates and the efficiency with which it rounds the wheels.
First the results emphasize the fact that the endplates are compulsory to get enough downforce: the efficiency of the two-element wing without any endplate is really poor. Thanks to all the devices and certainly mainly thanks to the vertical airfoil that limits the rounding of the horizontal airfoils tips by air, the downforce that the horizontal airfoils are able to produce is hold. However the drag is lower for this simplest geometry even if the gap is not significant (less than 5%). This difference is due to the large amount of downforce created in the more complicated geometries.

Then the geometries designed with the big vertical airfoil deflect more air from the wheel so that the drag produced by the latter is reduced compared to what may be expected.
Therefore the gap in downforce between the second model and the basic one is much higher than for the only front wing simulation. This difference is mainly due to the lift the rotation of the wheels creates as the gap between the two geometries is doubled with the k-ε viscous solver.

2. OBSERVED FLOW PATTERN

2.1 The multi-element airfoil

Thanks to the slope of the two-element airfoil along the span, the flow has greatly been improved. First the fact of setting a gap between the lower surface of the first element and the bottom of the vertical airfoil prevents the air from rounding the endplates as it was expected during the design process. This avoids the depression to be affected by the air rounding the tip from the high pressure –the upper surface- to the low pressure –the lower one-. Fig. 24 shows the velocity intensity at the multi-element airfoil surface: velocities are much higher along the wing span especially at the tip.

Then, the curvature of the wing at the middle of the span allows taking advantage of the ground effect and so to higher the downforce. The streamlines are closer to each other in this area. The wing works as a venturi with the ground and so creates more loads on the front wing (see Fig. 25, 26, 28, 29, 30 and 31). The suction at the centre of the span has an influence along the whole span on the lower surface as it is shown with the isobars from Fig. 29. Indeed the air on the lower surface has a trend to curve its path to the inboard direction much more than the one on the upper surface (see Fig. 32).

Finally, even if this is not the aim of this study and that the two elements of the front wing has not be made for each other, the GAW-1, the first one, feeds with air the lower surface of the second element quite well (see Fig. 30).

2.2 Vertical airfoils

The vertical airfoils definitely help the flow to take an inboard direction.
The flow on the inboard side of the vertical airfoil is of course deflected as it can not go through the airfoil. However, it is almost deflected upward because of the high incidence of the main wing second element.
Then the flow on the outboard side of the vertical airfoil is sucked inboard. The efficiency is highlighted thanks to the simulation provided by the basic model. This is easily seen on Fig. 33 and Fig. 34 as the velocity vectors take the inboard direction. However its efficiency is altered by the fact the air has to round the wheels and because of the superpressure in front of the tyres. Indeed, although a low pressure area would have been expected on the outboard side, the latter is ruled by a high pressure area when it gets closer to its trailing edge because of the proximity of the wheel.
So, air is sucked in the inboard direction from the leading edge of the vertical airfoil and then, when it gets closer to the wheel, the bypass of the wheel takes turn and favours this suction.

Although air seems to be well deflected inboard, this trend could be really improved. Indeed, it can be seen on Fig. 33 and Fig. 34 that air particles rounds the top tip of the vertical airfoil. Two factors are responsible for this flow disruption: the depression on the outboard surface of the vertical airfoil and the overpressure on the upper surface of the multi-element airfoil. Of course, air particles go from the high to the low pressure and create a wing tip vortex at the top of the NACA 68005.
Observing this phenomenon, the same flow pattern may have been found at the bottom of the same airfoil section. But the depression is so important on the lower surface of the multi-element airfoil that the suction from this location totally reverse the direction of the vortex, the air particles travelling from the outboard to the inboard surface of the vertical airfoil (see Fig. 33 and Fig. 34).

Finally one of the vertical airfoil great influences is to prevent the superpressure from the tyres to extent forward until the surfaces of the two-element airfoil (see Fig. 37). This allows protecting the loads created by the wing which is not the case in the wing without any endplate.

2.3 Flow over wheels / Horizontal flat plates

2.3.1 Wheel

Badly, the viscous solver used did not allow getting suitable results for the flow induced by the rotating wheels. The rotation of the wheel is simulated (see Fig. 38) but the resulted flow from CFD does not match with the one from some wind-tunnel tests made by previous research. To catch the separation that should have occurred, the length scale was reduced as well as the turbulence intensity but it does not change that much.

However, the pressure distribution (see Fig. 36) obtained shows the reason why the wheels are responsible for half of the drag of the car: the front of the tyre is a huge overpressure area –that extends quite far from ahead of the tyre (see Fig. 37)- whereas the back of it, dominated by recirculated flow, is a low pressure one retaining the car from moving forward. Fig.39 and Fig. 40 provide the evidence of the efficiency of the endplates in term of deflection of the flow. Indeed the distribution of pressure on the inboard side (left on Fig. 39 and Fig. 40) of the tyre shows lower pressure. That means that most of the flow has been sucked inboard by the endplates.
By comparing the different models, it appears that the Model 2 is more efficient than the Model 1 in term of drag. Apparently, the small NACA 68005 of the Model 1 is too close from the wheel and, as its angle of attack is too low, it forces air to take the direction of the wheel surface rather than deflecting it from the tyre (see Fig. 41 and Fig. 42). That is the reverse effect from the expected one.

2.3.2 Model 1

The first Model provides interesting results about its upper flat plate. From the leading edge of the vertical airfoil to the apex of the upper flat plate, the behaviour of the flow is of course the same as the basic model one. From this point to the appearance of the small vertical airfoil, two vortices are created. The first one, the strongest one is induced by the difference of pressure set by the vertical airfoil. The second one is a result of the first one: indeed, as the upper flat plate thickens the vertical airfoil upper tip, the flow rounding the tip (and creating the first vortex) induces a secondary vortex stuck to the upper

flat plate. As this creates a low pressure area and so lift instead of downforce (see Fig. 43), the rounding flow induced by the vertical airfoil has to be avoided.

2.3.3 Model 2

Fig. 44 and Fig. 45 show the difference between the basic model and the Model 2 velocity profiles at a height of 0.287m near the trailing edge of the vertical airfoil. Because of the inclined flat plate, the flow is accelerated on the latter's upper surface compared to the flow provided by the basic front wing. However the upper horizontal flat plate disrupts the flow and obliged air to bypass it by using the side way for some particles of air. This makes the flow intensify the high pressure on the wheel surface as these particles do not take benefit of being deflecting inboard of the wheel. For the second model, this small plate should be removed as well as it would not provide as much downforce as expected because of its small size.

2.4 Inclined flat plates

As expected, a vortex is created from the apex of the flat plate. So the angle of attack chosen -12 degrees- is sufficient to generate the resulted vortex and a flow separation at the leading edge (see Fig. 46, Fig. 47 and Fig. 48). However the vortex becomes flat close to the plate whereas it keeps its circular form at its bottom. So maybe the angle of attack might have been increased.

The vortex is rotating under the flat plate and therefore, as the speed of the air is higher thanks to the rotation of the flow, a low pressure area is created as expected (see Fig. 49 and Fig. 50). However, the low pressure surface does not extend until the trailing edge because of the disruption due to the wheel (see Fig. 52 where the pressure becomes higher and higher when the section gets closer to the trailing edge). Anyway the delta flat plate creates a low pressure surface and even if its effect is lowered by the wheel when approaching the trailing edge, it creates additional downforce and deflects the flow from the wheel very efficiently. Badly the difference of pressure between the upper and lower surface of the flat plate is also disrupted by the tip vortex from the vertical airfoil (see Fig. 48 and Fig. 51).

3. IMPROVEMENTS TO BE CARRIED OUT

This part gives directions to improve the second model or give new direction of designing the front wing. Some of them do not match each others and so it would permit to carry out several studies so that they would be compared.

3.1 The multi-element airfoil

First, to carry out studies with better accuracy, it should be better to get data from recent airfoils used in Formula 1.

The ride height of the front wing was set to 2.5 cm to get as much downforce as possible. Badly, this height is too low and should be increased to at least 6 cm so that the car would not be too sensitive to the pitch and to the side of the track when drivers try to get a tight path.

To get a significant gap between the lower surface of the first element and the bottom of the vertical airfoil from each endplate, the two elements should be twisted at their tip, keeping the same trailing edge height but so curving the leading edge to decrease the incidence at the tip locations. This would permit to help the endplates to prevent the air from rounding the first element tip from the high to the low pressure by keeping a minimum height of the same first element so that its ride height should be minimised along quite the whole span. It would also reduce the difference of pressure close to the tips. This would increase the ground effect too (and so the downforce) as the ground clearance will be reduced along most of the span. However, a straight element may be preferred if the aim is to suck air from outboard (see the end of 3.4)

3.2 Vertical airfoils

First, the small airfoil, even if it has not be tested on the second model, may be abandoned as it has not shown a great influence on the first model (see Fig. 41 and Fig. 42). Otherwise, if it is kept, its angle of attack may be increased to at least 30 degrees because of the influence of the wheel and it should be set ahead so that it would deflect the air flow before reaching the superpressure area. In this case, the aim of this small airfoil would be to dilute the superpressure located on the wheels and maybe to decrease drag but it would

not be significant. This would in fact transfer some drag from the tyre to the front wing.

To allow more air to be deflected inboard the wheels, the vertical NACA 68005 airfoil should be twisted at its bottom near its trailing edge to increase the gap between the tyre and this airfoil. A greater amount of air may be deflected in this gap so that less air would have to hit the tyre and so a gain in drag may be obtained.

Then, as the air rounding endplates at their bottom (because of the difference of pressure between the outboard side of the NACA 68005 and the lower surface of the multi-element airfoil) would not affect the second element that much, an additional small horizontal airfoil (with a chord of around 10 to 15 cm) may be added at the trailing edge of the endplates on the inboard side to suck air from the external side of them to the internal one. This would help the flow to be deflected inboard again, to prevent this air to reach the tyre and so again to avoid useless drag.

To avoid the wing tip vortex at the top of the vertical airfoil, a winglet may be added at the top of the vertical airfoil. It should be done inboard (at 0.3 metre above the reference plane, i.e. at the limit allowed by the regulation or by following the airfoils' elements upper surface shape to drive the air) and outboard.

Finally, it should be interesting to see the difference between a vertical airfoil curved in the other direction. Of course, the solution may be guessed and so maybe an adaptive curvature may be chosen by the designer so that he could produce the low and high pressure area at the place he wishes them. Therefore, it could be possible to control the vortex at the tips (so at the top and at the bottom) of the NACA 68005 by playing with the tip curvature of the vertical airfoil.

3.3 Flow over wheels / Horizontal flat plates

The aim here is to take advantage as much as possible of this high pressure zone even if does not seem that easy.

A flat plate should be designed from the top of the vertical airfoil to the downstream and outboard limit allowed by the regulation (something that looks like the upper flat plate from the first geometry designed). In this way, air rounding the vertical airfoil by the top would be limited and taking advantage of the induced flow from the rotating wheel would still be possible. Therefore it would not disrupt the inclined flat plate and its resulted vortex if the height of this one is reduced as described in one of the following part.

3.4 Inclined flat plates

As the vortex becomes flat when it gets close to the lower surface of the inclined flat plate, it should be tested by a higher angle of attack. Therefore maybe the fact that the vortex core is closer to the plate induces higher speed (and so a lower pressure area) next to the lower surface as the core is closer to the surface. However, the vortex might get slower because of the friction next to the lower surface of the flat plate.

Then, as the vortex flow is disrupted by the flow from the rotating wheel and that the latter induces high pressure area at both upper and lower surface of the flat plate, the downforce created by the flat plate would be risen if it was set closer to the ground as the wheel is further at this location (as it is round!). However, it should not be too close as the suction from the multi-element airfoil may destroy the vortex. To keep the depression of the multi-element airfoil from bursting the vortex, the vertical airfoil may be curved outboard at its bottom so that the suction from the multi-element wing will not affect the vortex (the same principle as the one from Fig. 20).

Another way to improve this device would be to higher the vortex size. To perform this improvement, the flat plate leading edge should extent in width. This would imply to cut the vertical airfoil just upon the upper surface of the first element of the two-element wing. However, this will not alleviate the downforce provided by the multi-element airfoil too much as it would only affect the superpressure upon it. The design would have to be smooth as the aim is to prevent the formation of vortices but the one from the flat plate.

As the flat plate would be curved with a negative angle of attack, it would be possible to retrieve the whole shape of the vertical airfoil close to the trailing edge.
If this way of designing the inclined flat plate is done, it should be useful to study the effect of extending the flat plate until the trailing edge of the vertical airfoil. This would permit to create more downforce but this may be doubted because of the overpressure due to the wheel in this region. Otherwise, the flat plate could be cut sooner with a greater angle of attack to deflect the flow up more efficiently.

Badly, the previous feature may not be compatible with an inclined flat plate set close to the ground. However an inclined flat plate is not required to create vortex that are able to create vortex lift thanks to the high speed induced by the rotating flow. A flat plate at a zero angle of attack may be sufficient if the designer uses the flow rounding the endplates thanks to the enormous difference of pressure between the several locations around the front wing.
For example, a flat plate (No.1) might be set along the whole chord of the vertical airfoil on its outboard side. This airfoil may get a winglet (No.2) (that should be curved to make the bypass of the flow easier) at its exterior edge to allow the presence of a high –or at least not a low one- pressure area (No.3). Above the latter, the flat plate (No.1) –which would be the one that carries the additional downforce- would induce the creation of a vortex that may develop below it.

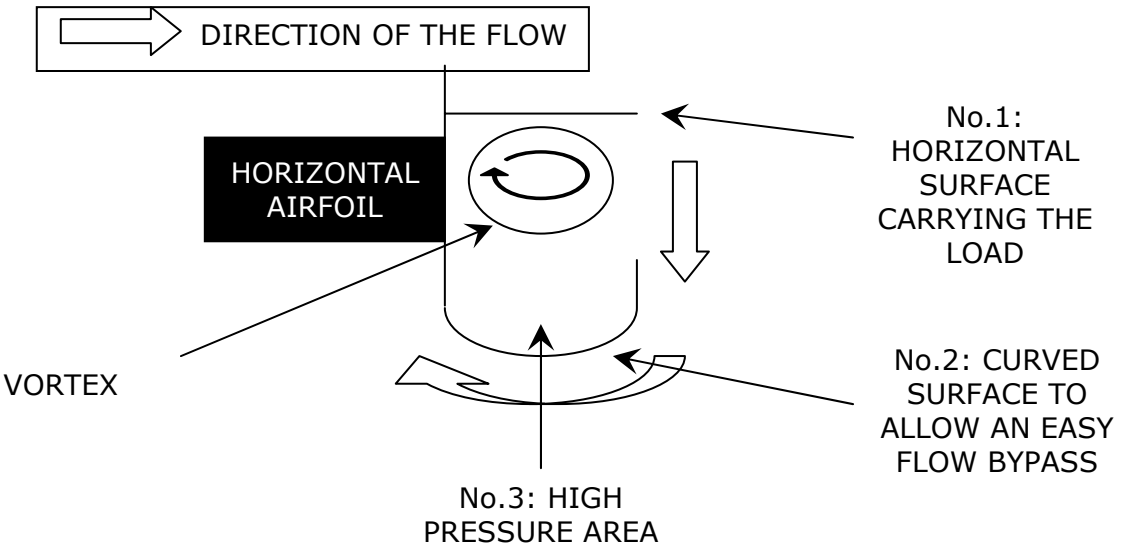

Fig. 20: Creating a vortex using the multi-element airfoil suction

To conclude, if new studies from this work are carried out, it may be interesting too to get several models as it was done here to be able to assess the efficiency of each device.

This chapter "Improvements to be carried out" shows many ways to create new models. Of course, the list of ideas listed here is not exhaustive. This means that there are still many ways to improve the front wing and that many studies will still be carried out.

CONCLUSION

This thesis includes three main steps: designing geometries, meshing them and analysing them.
The design part which is very interesting was complicated to carry out. However the link between the design part and the mesh part has to be done carefully. Indeed the design has to be often modified to clean the geometries so that no extra and useless edges may occur in the grid generation software. This makes the meshing step easier and it becomes a gain of time during the grid generation process which is the longer to carry out. Then, the simulation runs after picking the right solvers and settings. Finally the analysis permits to confirm the design, to modify it, to improve and to find new devices that would be used to undertake another loop.

The loop carried out in this thesis deals with three geometries. The first one assessed the contribution of the vertical airfoil that is present in the two other geometries as well. The vertical airfoil permits to deflect air from the front wheels and so to reduce the drag. It also prevents the superpressure from the wheel to extent until the multi-element airfoil surfaces which is the most important downforce creating device.
The low curvature of the multi-element horizontal airfoil was assessed and the gain due to the ground effect appears to be quite important.

Then the Model 1 was built to evaluate the small vertical NACA 68005 close to the wheel. This airfoil is not useful as the flow already rounds the wheel by itself at this location. So if this device remains, it should be attached forward on the front wing and should get a higher angle of attack to divert air more than the wheel does.

Finally, additionally to deflect the air from the wheels, the Model 2 endplates create downforce thanks to the vortex (negative) lift created by the inclined flat plate. The expected additional load has been created even if it was hoped to be bigger.

This study permits to run simple front wing shapes with CFD, to assess them and to imply new design. Although the FIA Formula 1 technical regulation sets a lot of constraints, maybe the latter is the engine of aerodynamics research in Formula 1.

BIBLIOGRAPHY

Renaud de Laborderie, Jean-Louis Moncet and Giorgio Piola, (March 1991 to March 2003). *Revue de détails* in *Sport-Auto No 351* to *No 500*. Emap France, Paris.

Katz J., (1995). *Race Car Aerodynamics: Designing for Speed.* Bentley Publishers, Cambridge (USA).

Mortel F., (2002). *L'aérodynamique dans l'automobile*. Memoir for the U.T.B.M. (University of Technology of Belfort-Montbéliard). Citing Internet ressources (WWW document). http://site.voila.fr/mortelfl/ht02.pdf (accessed 15th may 2003)

Katz J., (1985). *Investigation of Negative Lifting Surfaces Attached to an Open-Wheel Racing Car Configuration.* SAE Report No 850283.

Fackrell J.E. and Harvey J.K., (1974). *The aerodynamics of an Isolated Road Wheel* in Proceedings of the Second Symposium on Aerodynamics of Sports and Competition Automobiles, (1975). Collection of AIAA papers by Pershing Bernard, Western Periodicals Co., North Hollywood, CA.

Stapleford W. R. and Carr G. W., (1970). *Aerodynamic characteristics of exposed rotating wheels*, Reports MIRA/AIC-1970/2.

Katz J. and Largman R., (1989). *Experimental study of the aerodynamic interaction between an enclosed-wheel racing-car and its rear wing* in Transactions of the ASME-Journal of Fluids Engineering, vol. 111, no. 2, p. 154-159, 1989. American Society of Mechanical Engineers, New York.

Katz J., (1995). *High-lift wing design for race-car applications* in The Journal of Passengers cars vol.104 part 2, SAE Paper 951976. Los Angeles.

REFERENCES

1. Florent MORTEL. *Photographies made at Donington Park Museum*. 17th February 2003.

2. Pierre Ménard, (2000*). The Great Encyclopedia of Formula 1, 1950-1999: 50 years of Formula 1*. London, Constable and Robinson.
   Or : Pierre Ménard, (1999*). La grande encyclopédie de la formule 1, 1950-1999: 50 ans de Formule 1*. Chronosports Editeur.

3. Renaud de Laborderie, Jean-Louis Moncet and Giorgio Piola, (March 1991 to March 2003). *Revue de détails* in *Sport-Auto No 351* to *No 496*. Emap France, Paris.

4. Jean-Eric Raoul (August 2003). *La mémoire de Sport-Auto: Jim Hall*. Sport-Auto No 499. Emap France, Paris.

5. Howard K. (September 2000). *Gurney Flap*. Edition of Motorsport magazine , England. Cited in: Dan Gurney's All American Drivers Online (WWW document) http://www.allamericanracers.com/gurney_flap.html (accessed 14th may 2003).

6. Florent MORTEL. *Photography made at Cranfield University*. May 2003.

7. FIA 2003 Formula One Technical Regulations.
   FEDERATION INTERNATIONALE DE L'AUTOMOBILE
   8, Place de la Concorde - 75008 Paris - France

8. FIA 2003 Formula One Sporting Regulations.
   FEDERATION INTERNATIONALE DE L'AUTOMOBILE
   8, Place de la Concorde - 75008 Paris – France

9. Fackrell J.E. and Harvey J.K., (1974). *The aerodynamics of an Isolated Road Wheel* in Proceedings of the Second Symposium on Aerodynamics of Sports and Competition Automobiles, (1975). Collection of AIAA papers by Pershing Bernard, Western Periodicals Co., North Hollywood, CA.

10. *Tyre for dry surface ("grooved tyre")*. Cited in: Michelin F1 web site (WWW document). http://www.michelinf1.com/content/xml/pneu_popup1_en.xml (accessed in june 2003)

11. Pointwise, Inc.-Fort Worth, Texas–United States of America. *Gridgen User Manual*. Accessed on line.

12. Fluent Europe Ltd-Sheffield business park-Europa link-Sheffield-S9 1XU-England, (2003). *Fluent 6.0 User's Guide*. Accessed on Cranfield University web site.

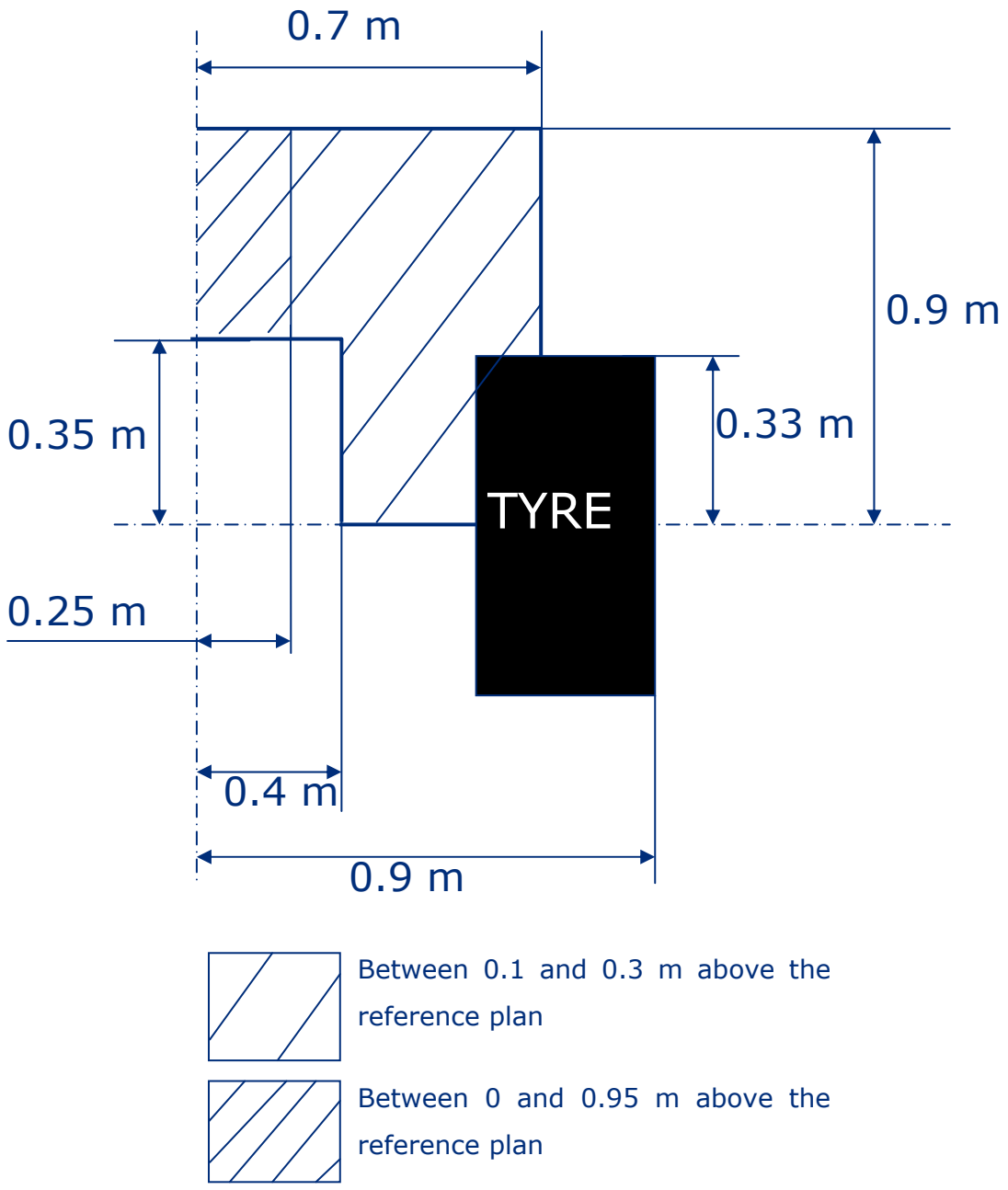

Fig. 21: FIA F1 technical regulation requirements

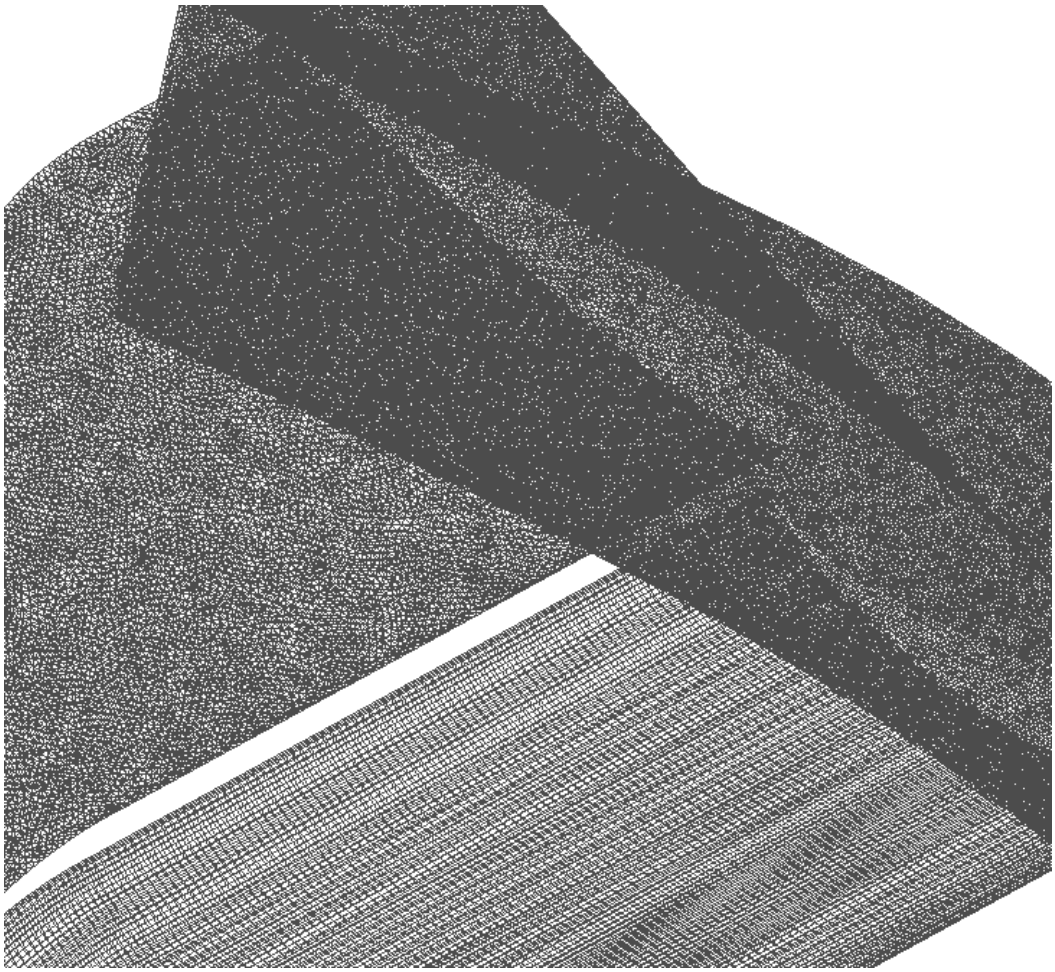

Fig. 22: Model 2 mesh

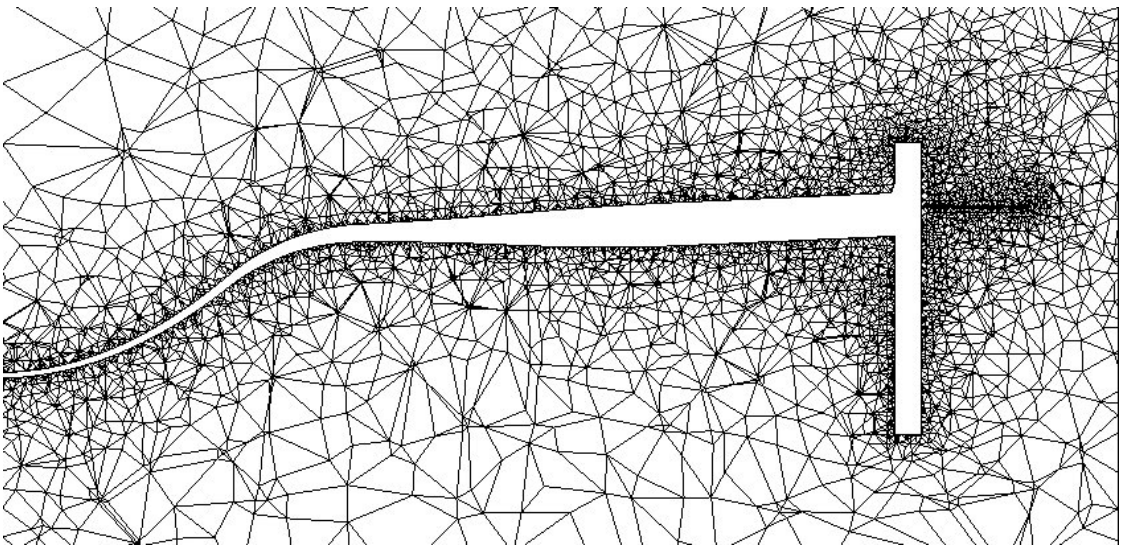

Fig. 23: Model 2 mesh along the plane at 0.4m from the leading edge

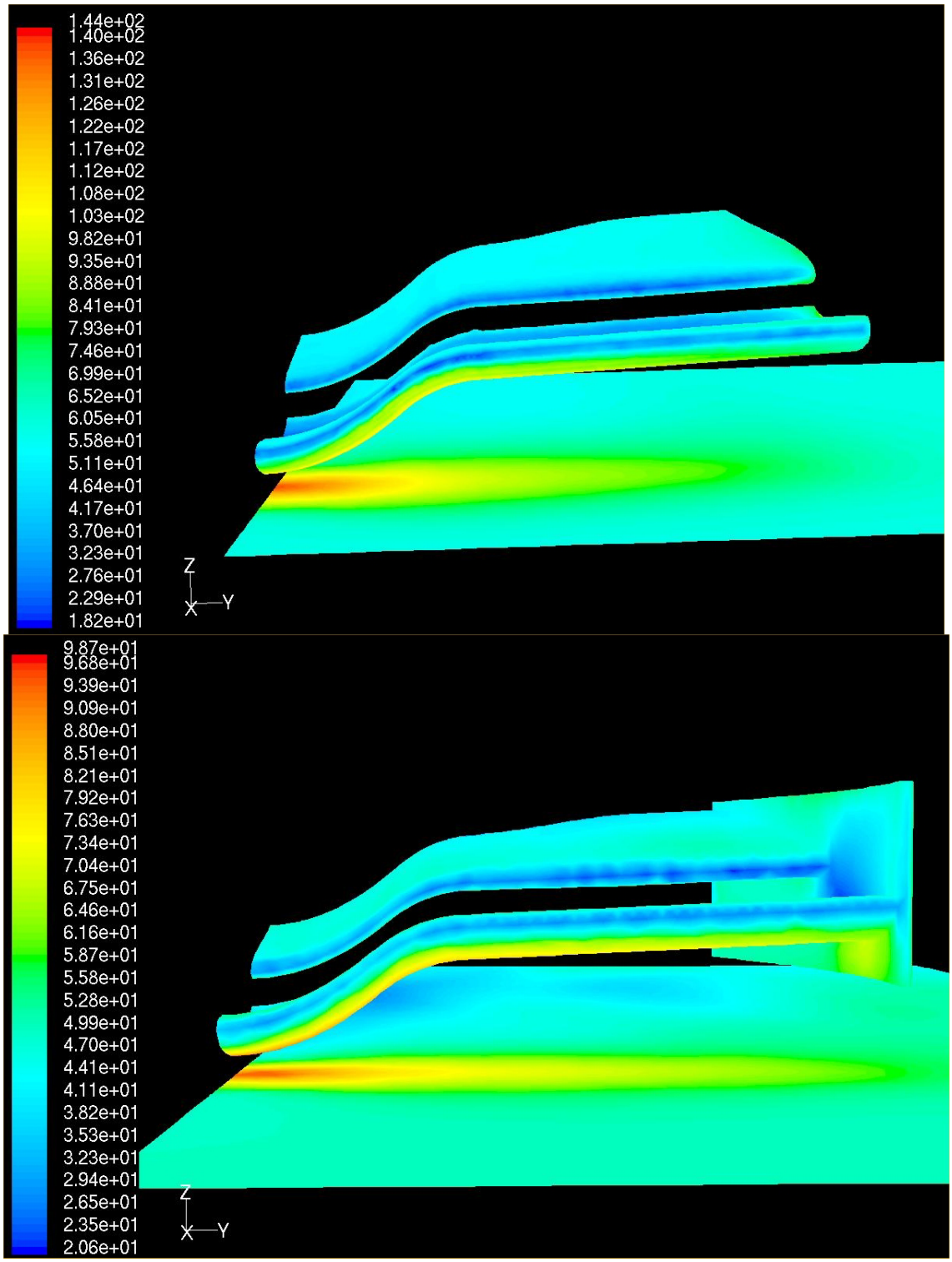

Fig. 24: Evidence of the endplates efficiency with velocity contours

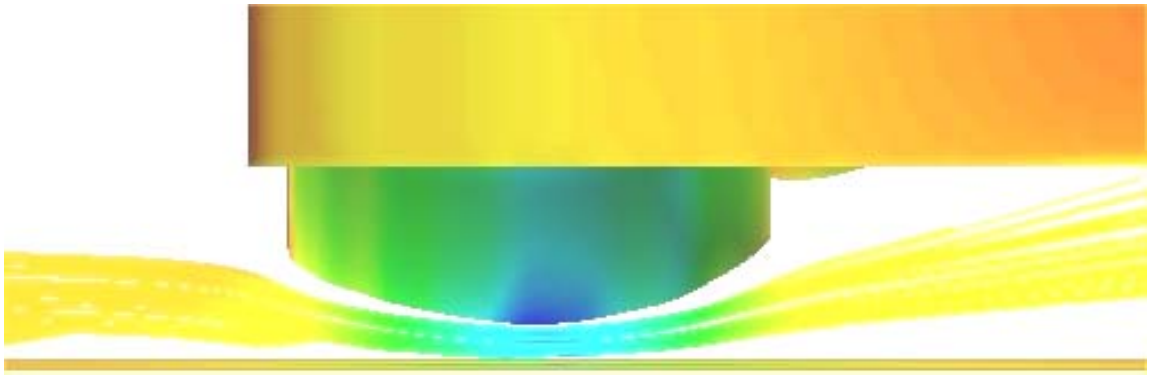

Fig. 25: Venturi effect near the centre line (Basic model)

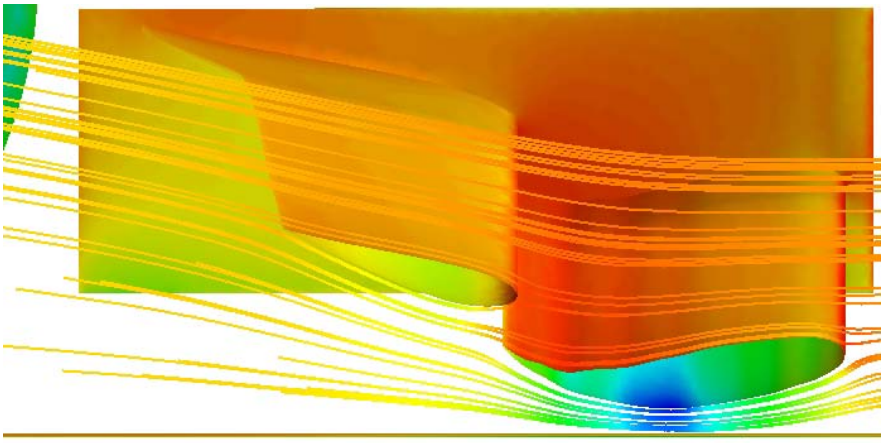

Fig. 26: Flow around the two-element airfoil

Fig. 27: Pressure distribution at 18cm from the leading edge

Fig. 28: Pressure distribution at 5 cm from the centre line

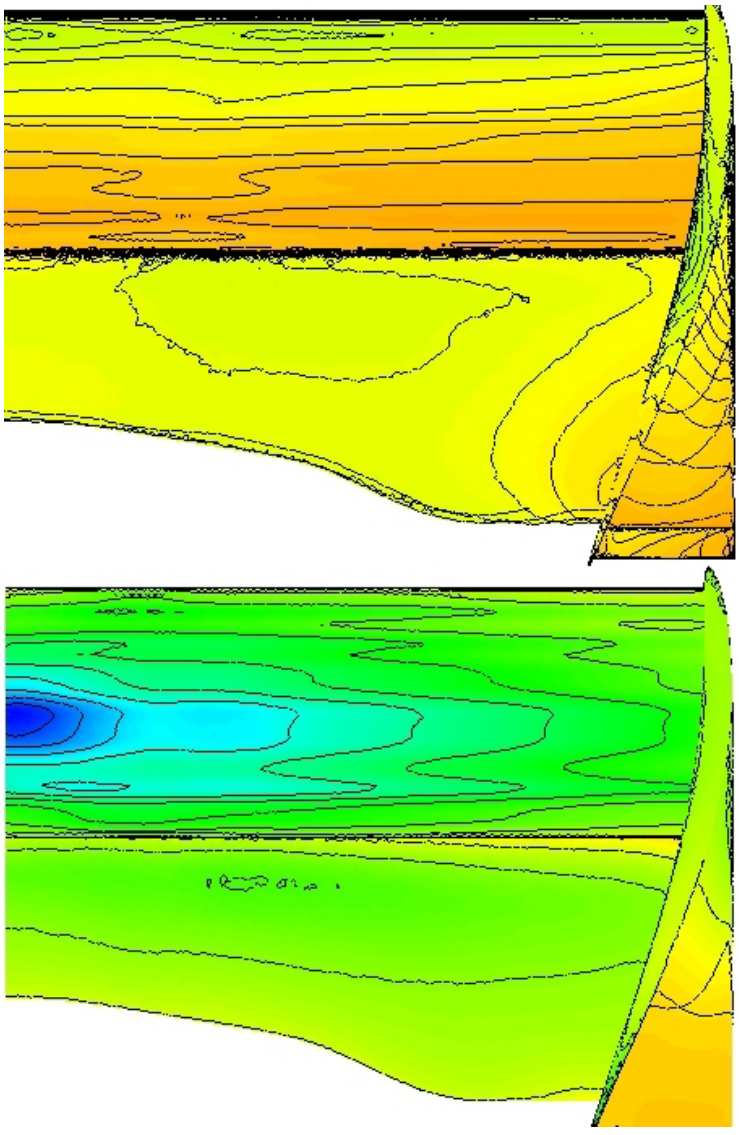

Fig. 29: Pressure distribution (including the isobars) around the two-element airfoil

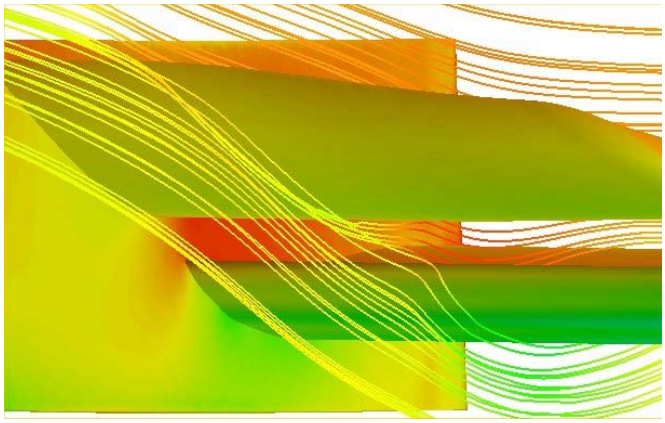

Fig. 30: The first airfoil section feeding the second one

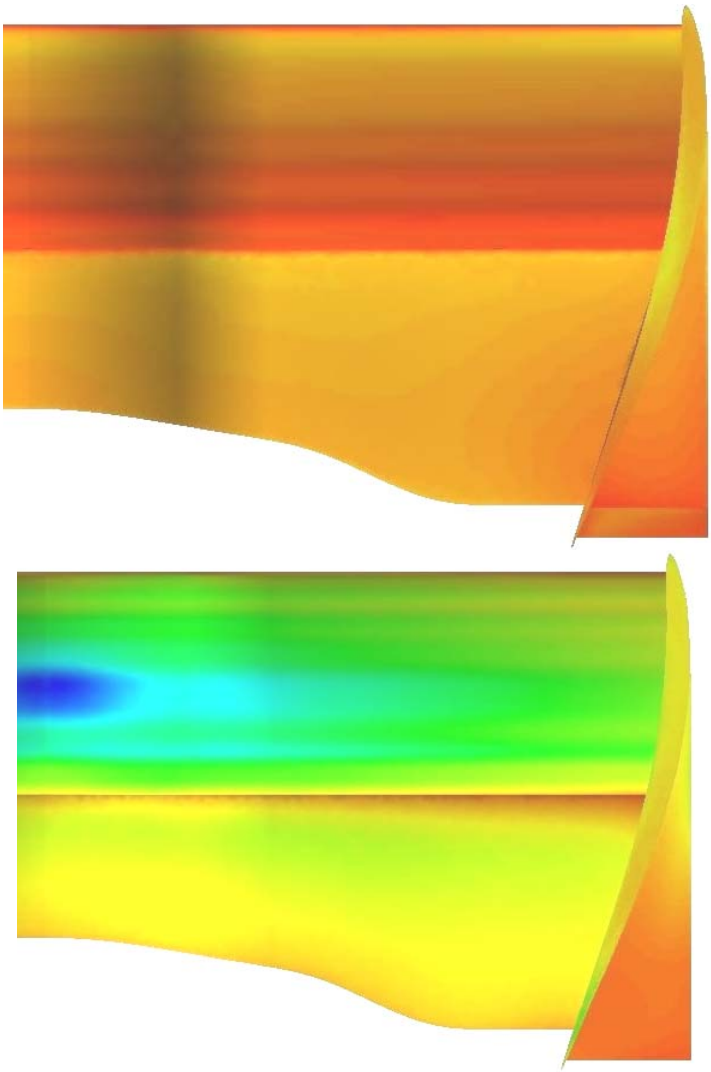

Fig. 31: Top and bottom view showing the pressure distribution on the multi-element airfoil

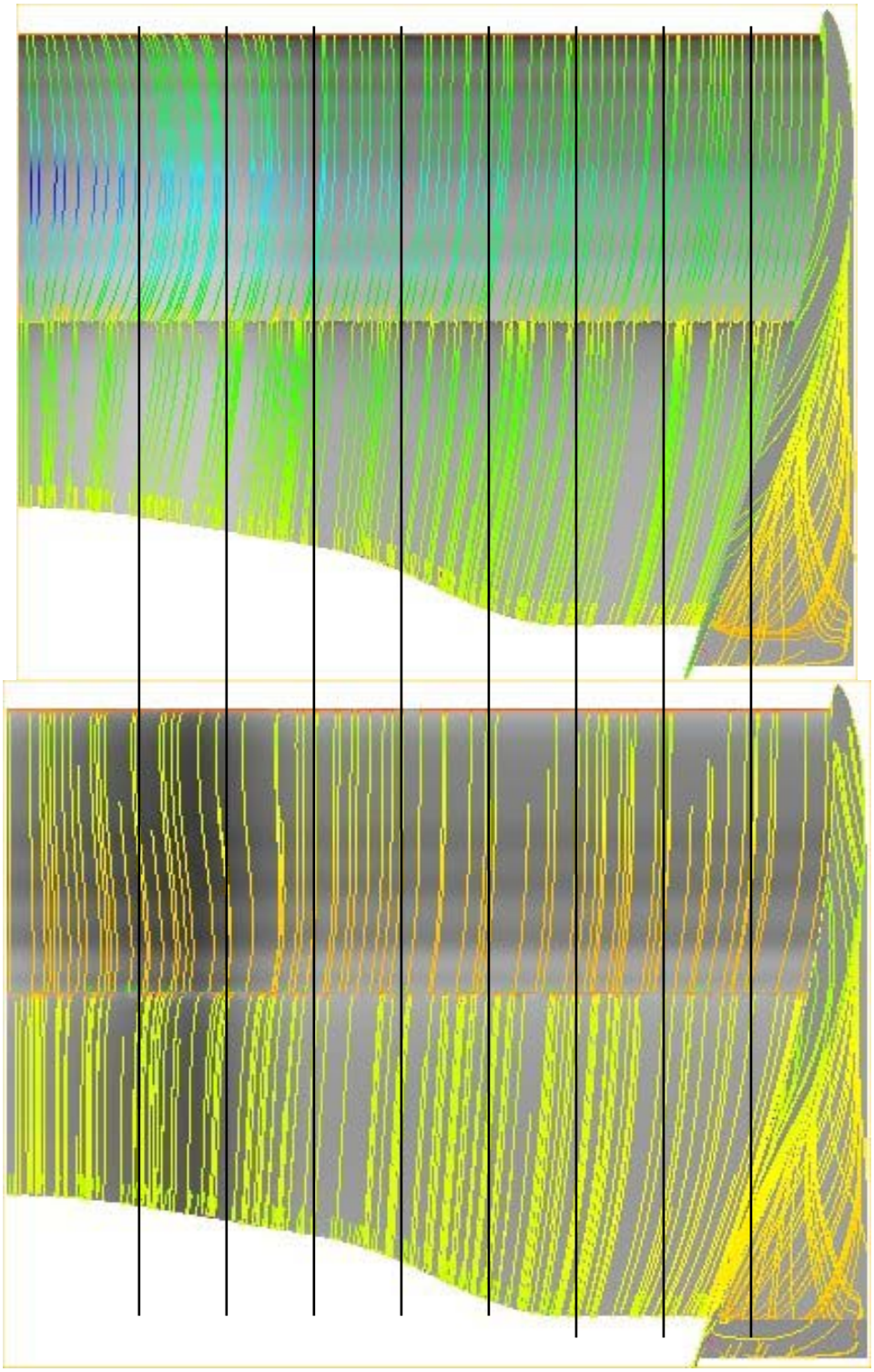

Fig. 32: Bottom and top view of the front wing with the surface flows colored by static pressure

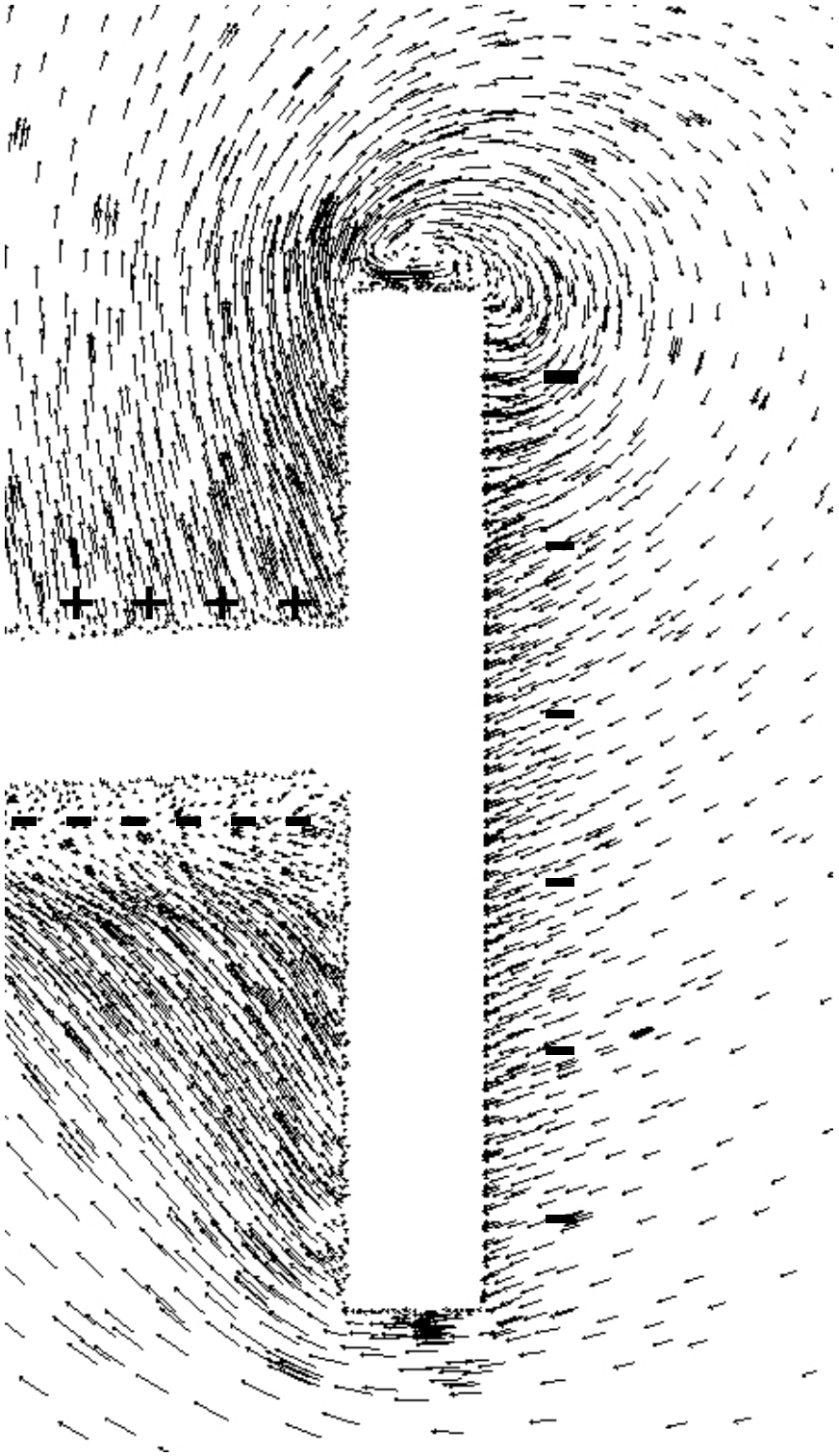

Fig. 33: Velocity vectors showing the vortex due to the vertical airfoil shape at 20cm from the leading edge (Basic Model / SA)

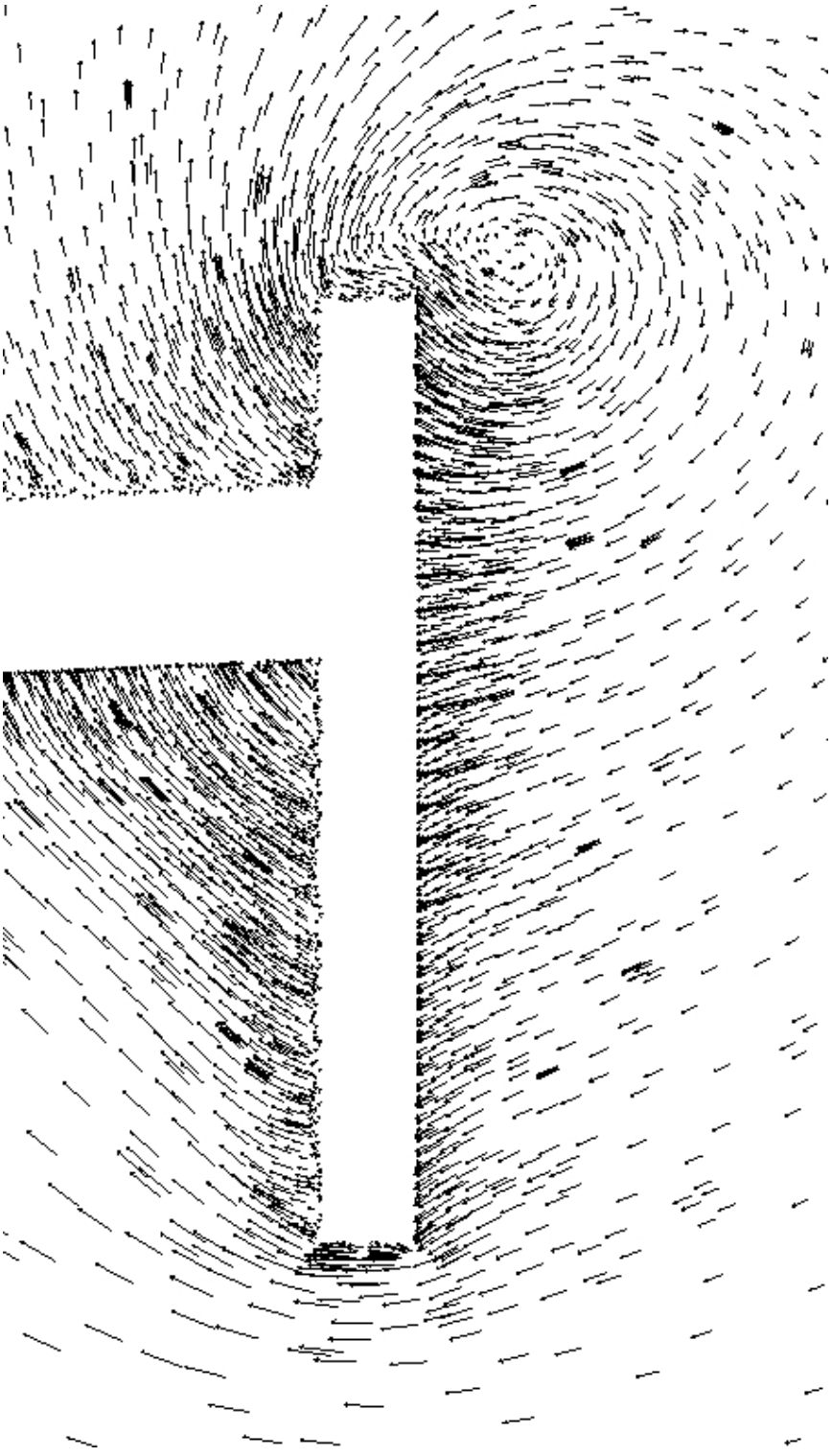

Fig. 34: Velocity vectors showing the flow induced by the suction from the vertical airfoil (Basic Model / SA)

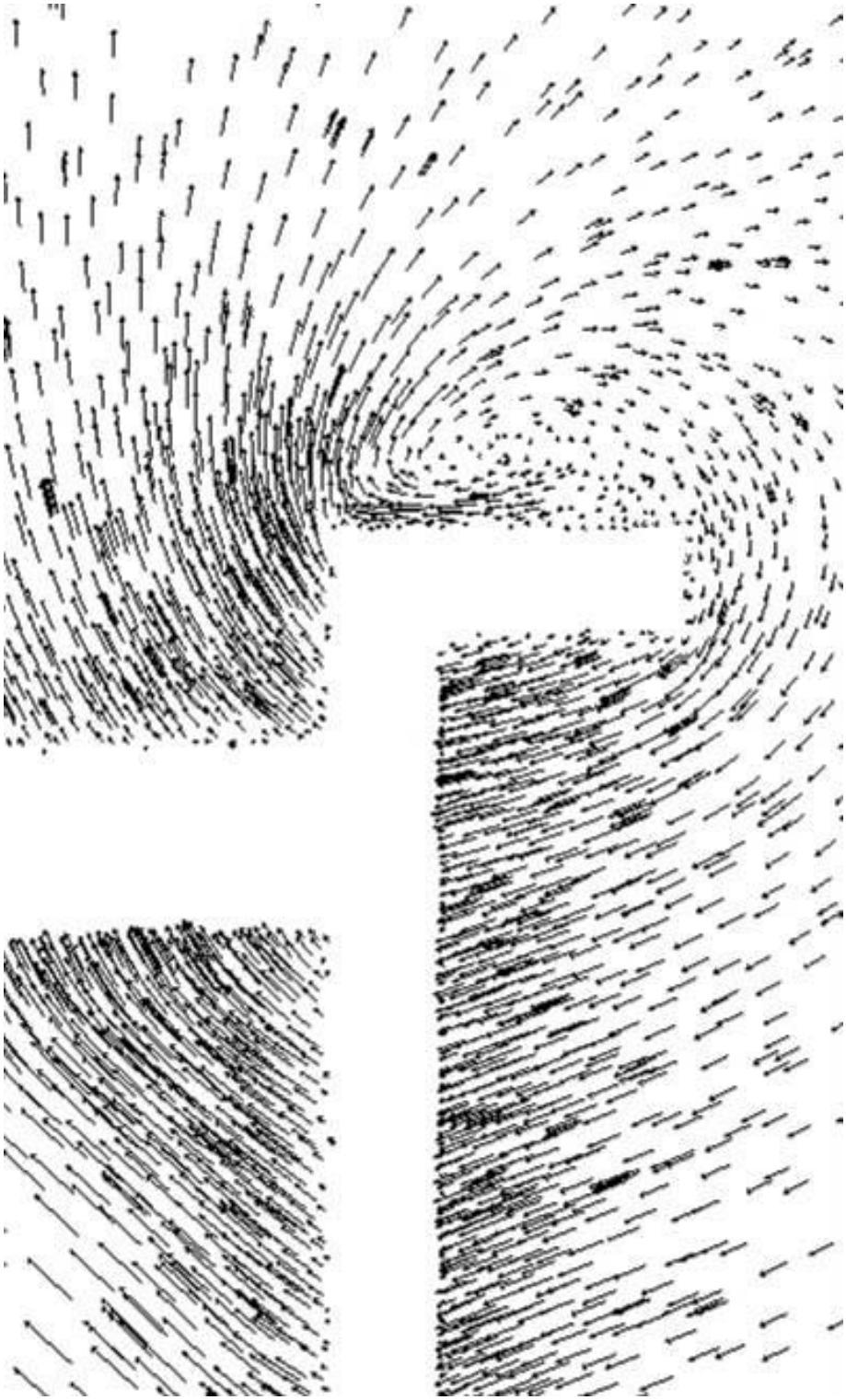

Fig. 35: Velocity vectors showing the secondary vortex on Model 1 at 33 cms from the leading edge

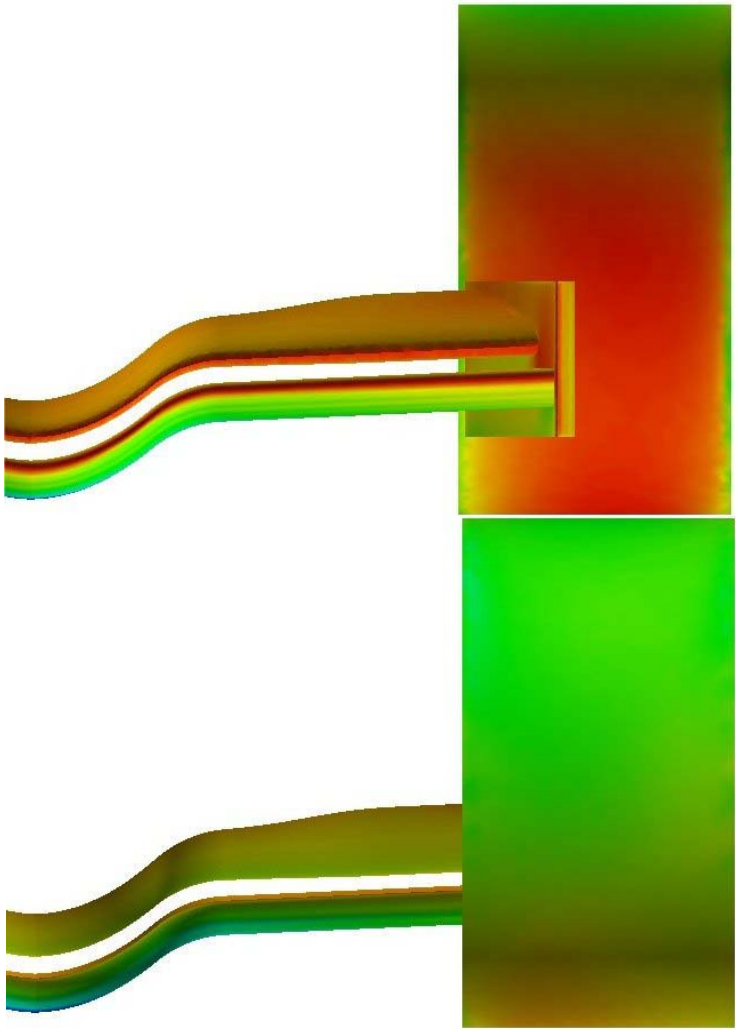

Fig. 36: Pressure distribution from the front and behind views

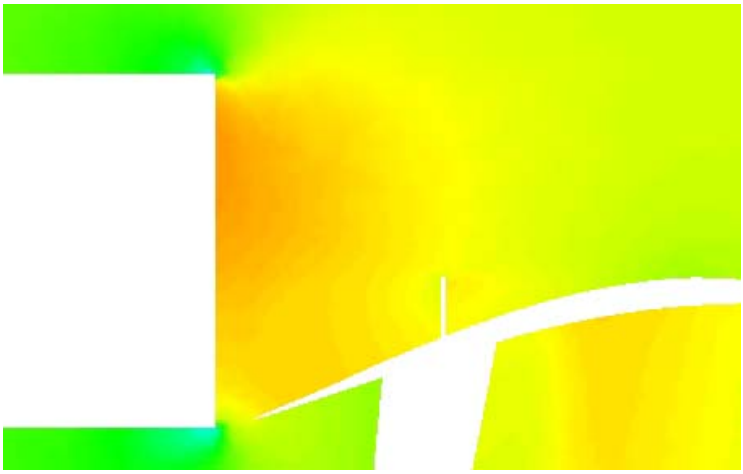

Fig. 37: Pressure distribution at z=0.25m (Model 2)

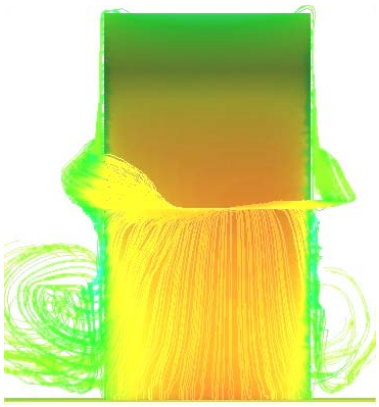

Fig. 38: Evidence of the rotating flow around the wheel

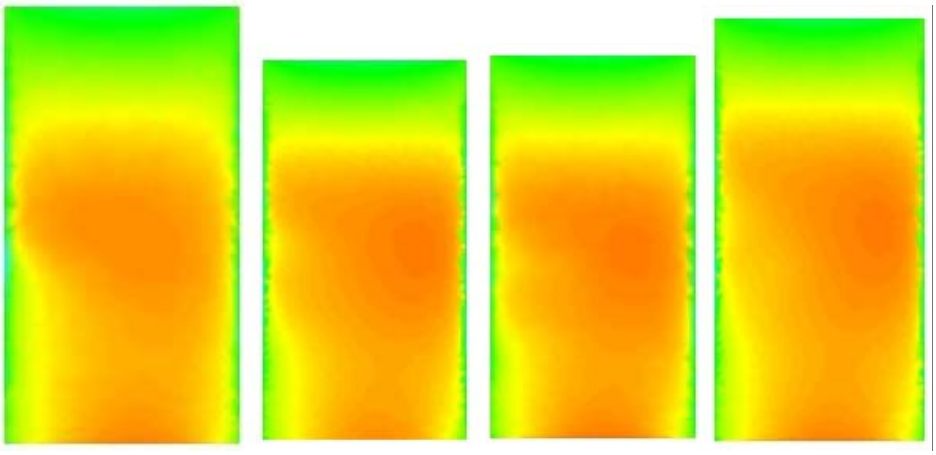

Without any tip **Basic model** **Model 1** **Model 2**

Fig. 39: Pressure distribution on wheel surface

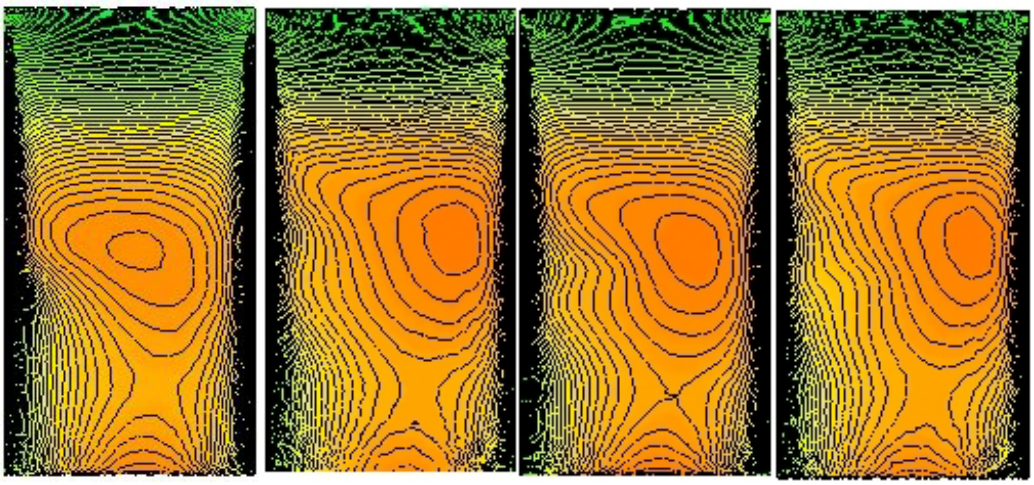

Without any tip **Basic model** **Model 1** **Model 2**

Fig. 40: Pressure distribution on wheel surface with isobars

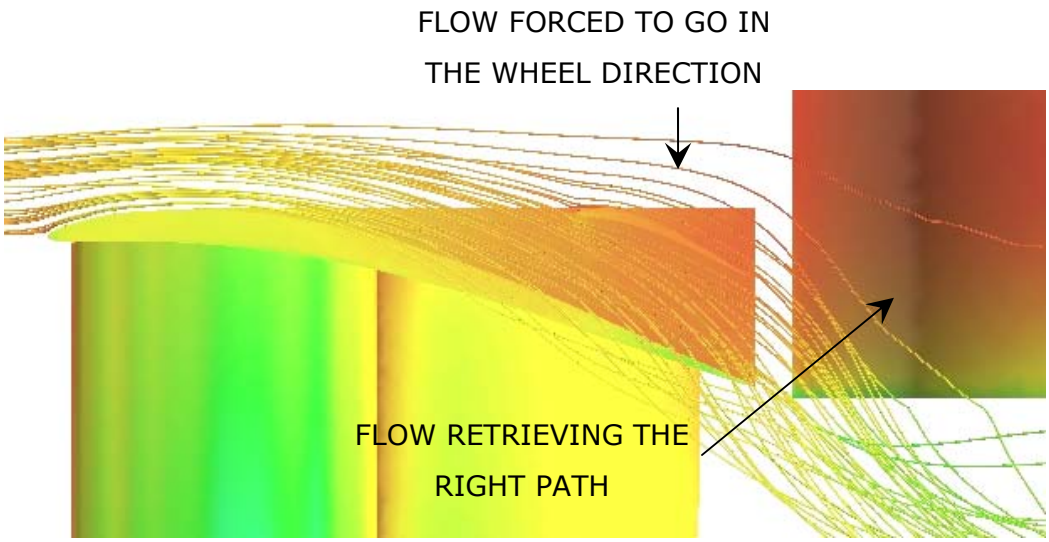

Fig. 41: Bottom view from Model 1

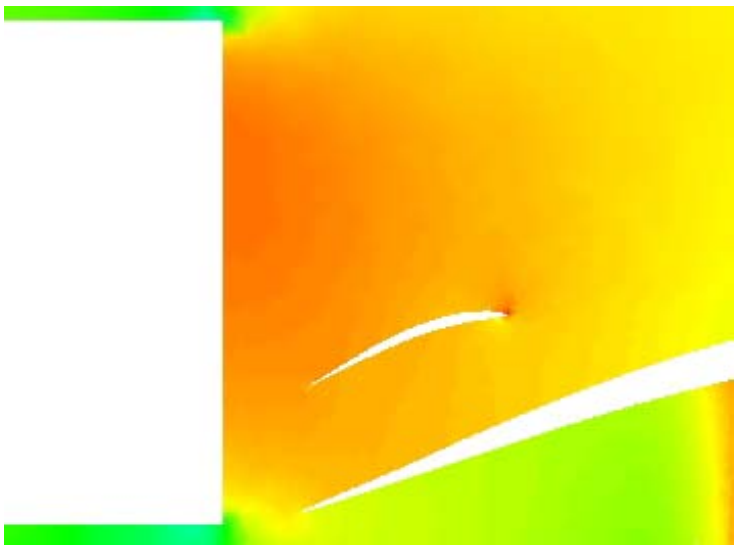

Fig. 42: Pressure distribution around the small NACA 68005 (Model 1)

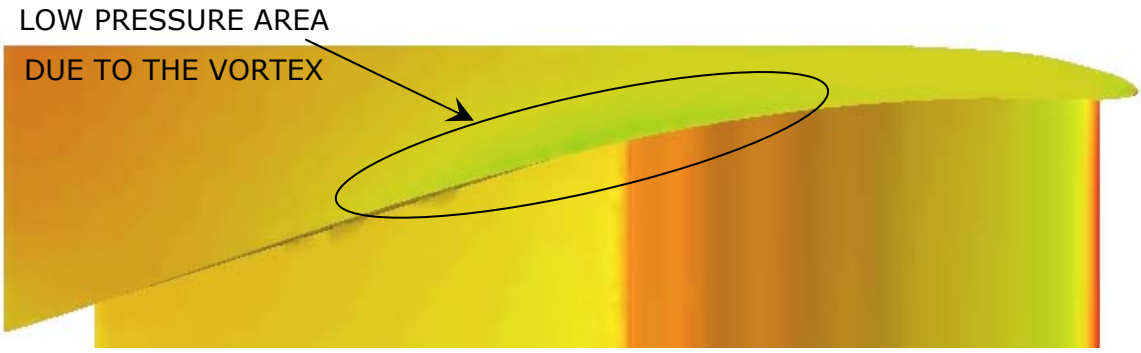

Fig. 43: Low Pressure due to the secondary vortex (1st Model)

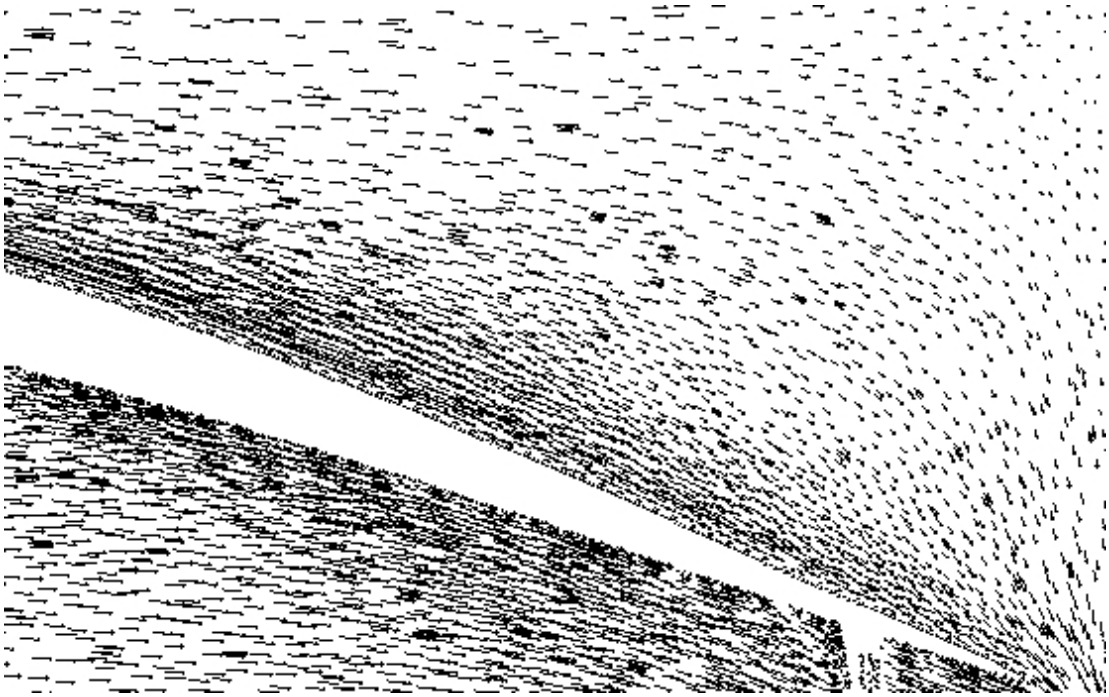

Fig. 44: Flow at the trailing edge of the vertical airfoil

(Basic model z=0.287m)

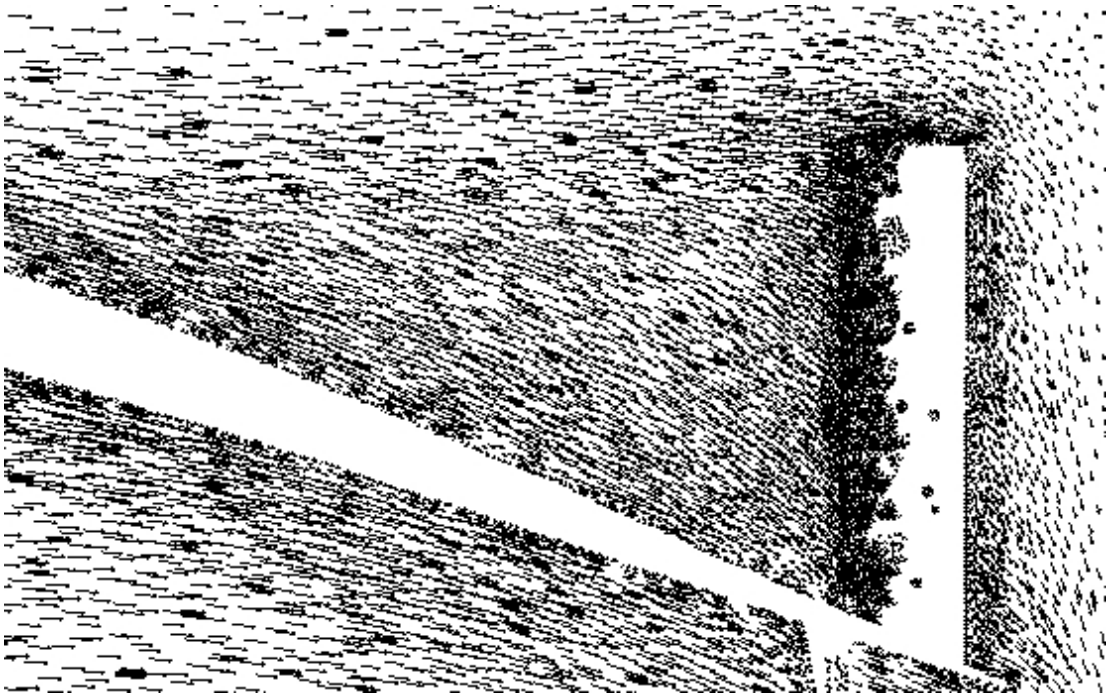

Fig. 45: Upper horizontal flat plate disrupting the flow

(Model 2, z=0.287m)

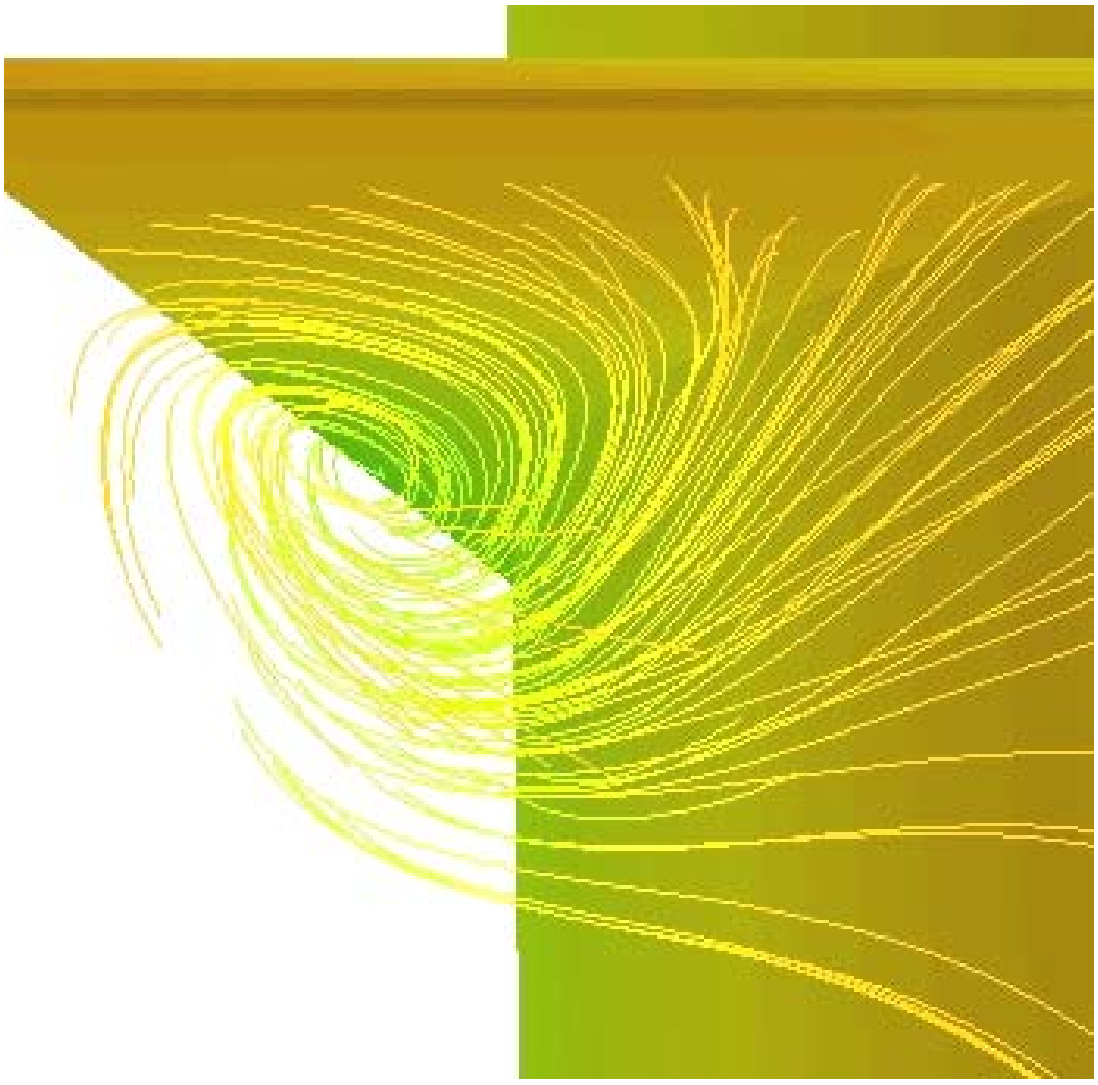

Fig. 46: Vortex created by the inclined flat plate (2nd Model)

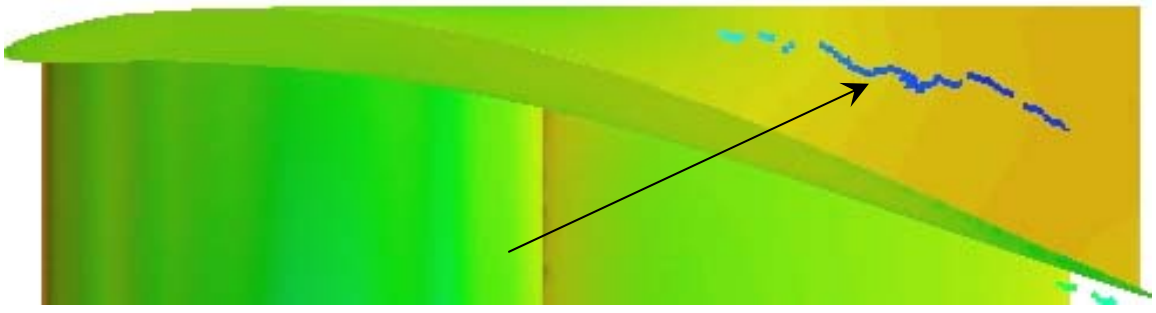

Fig. 47: Vortex axis

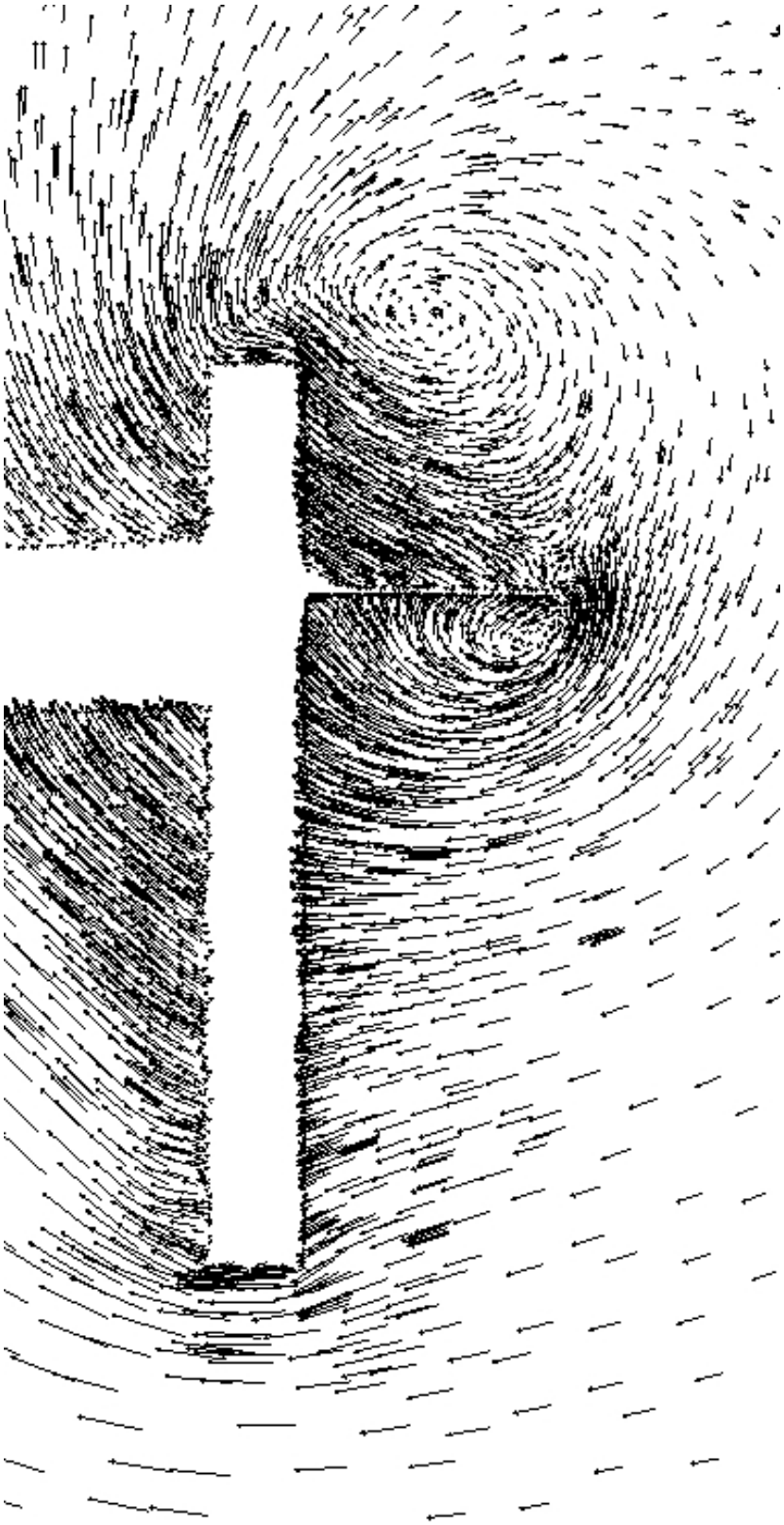

Fig. 48: Velocity vectors showing the vortices at 35 cm from the leading edge (2nd Model)

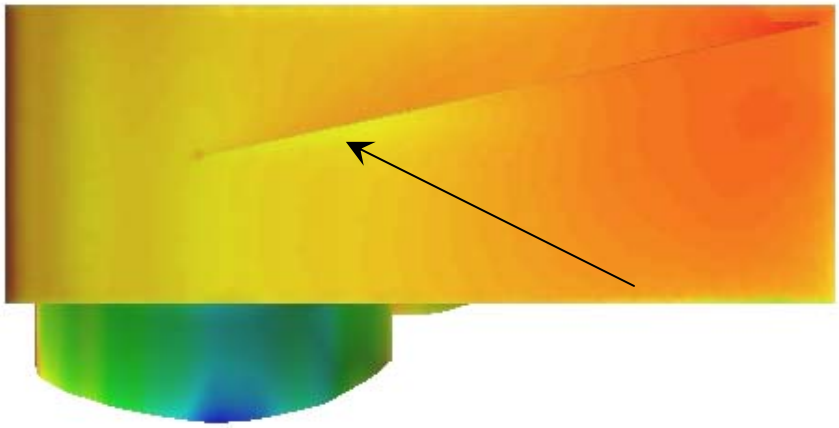

Fig. 49: Side view showing the low pressure area due to the vortex (Model 2)

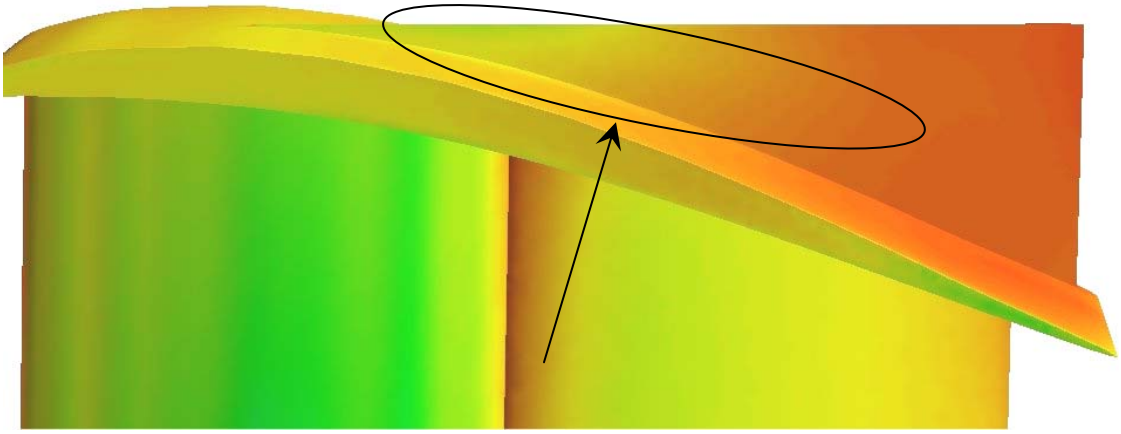

Fig. 50: Bottom view of the front wing showing the low pressure area due to the vortex (Model 2)

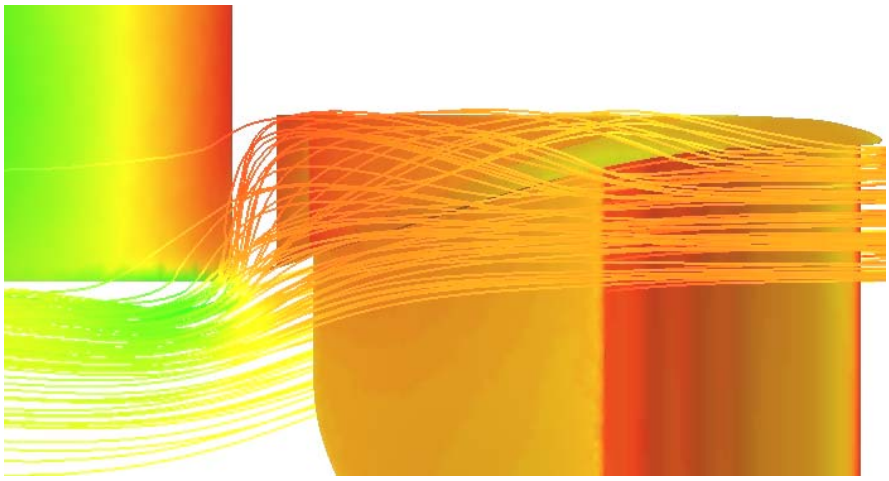

Fig. 51: Flow rounding the upper tip of the vertical airfoil (Model 2)

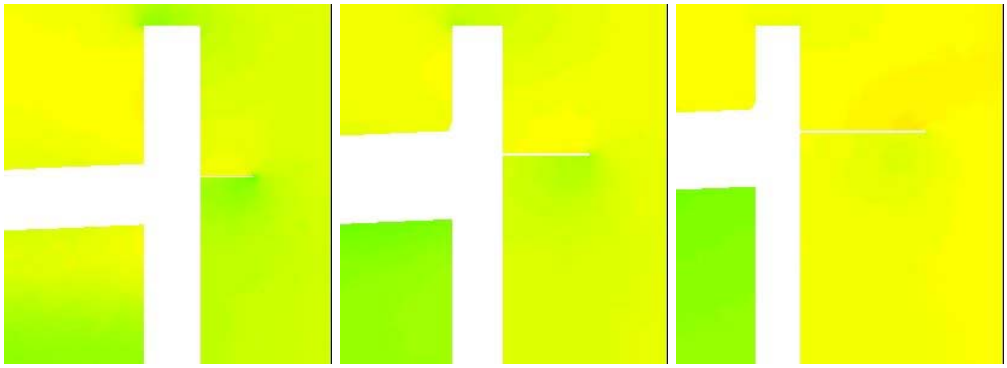

0.25m 0.3m 0.35m

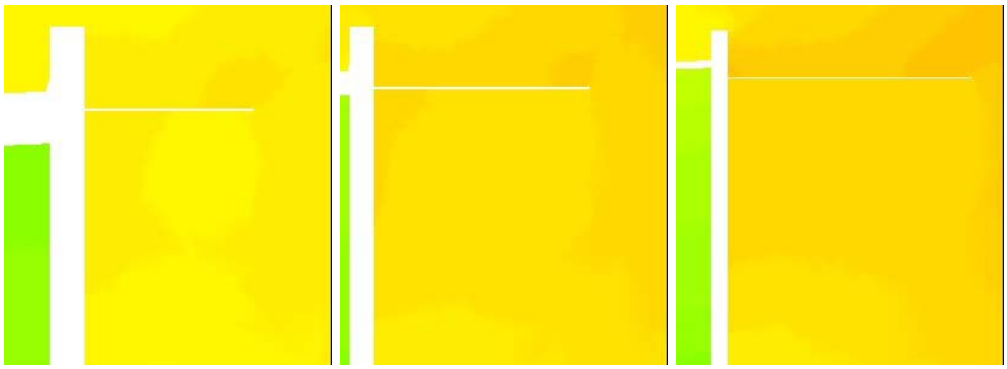

0.4m 0.45m 0.48m

Fig. 52: Pressure distribution along the chord of the inclined flat plate (distance are measured from the leading edge)